A new comparison of marine dispersion model performances for Fukushima Dai-ichi releases in the frame of IAEA MODARIA program

Raúl Periáñez [a, *], Igor Brovchenko [b], Celine Duffa [c], Kyung-Tae Jung [d], Takuya Kobayashi [e], Fernando Lamego [f], Vladimir Maderich [b], Byung-Il Min [g], Hartmut Nies [h], Iolanda Osvath [i], Maria Psaltaki [j], Kyung-Suk Suh [g]

[a] Dpt Física Aplicada I, ETSIA, Universidad de Sevilla, Ctra Utrera km 1, 41013, Sevilla, Spain
[b] Institute of Mathematical Machine and System Problems, Glushkov av., 42, Kiev, 03187, Ukraine
[c] IRSN, PRP-ENV/SESURE/LERCM, La Seyne sur Mer, France
[d] Korea Institute of Ocean Science and Technology, 787 Hean-ro, Sangnok-gu, Ansan-si, Gyeonggi-do, 426-744, Republic of Korea
[e] Japan Atomic Energy Agency, 2-4 Shirakata Shirane, Tokai, Ibaraki, 319-1195, Japan
[f] Instituto de Engenheria Nuclear, Rua Hélio de Almeida 75, Ilha do Fundão, CEP 21941-906, Rio de Janeiro, Brazil
[g] Korea Atomic Energy Research Institute, Daedeok-Daero 989-111, Yuseong-Gu, Daejeon, Republic of Korea
[h] Bundesamt fuer Seeschifffahrt und Hydrographie, Wüstland 2, 22589, Hamburg, Germany
[i] IAEA Environment Laboratories, 4a Quai Antoine 1er, MC-98000, Monaco
[j] National Technical University of Athens, Iroon Polytexneiou 9, 15780, Zografou, Greece

A B S T R A C T

A detailed intercomparison of marine dispersion models applied to the releases from Fukushima Dai-ichi nuclear power plant was carried out in the frame of MODARIA program, of the IAEA. Models were compared in such a way that the reasons of the discrepancies between them can be assessed (i.e., if they are due to the hydrodynamic part, the dispersion part, and the ultimate reasons). A sequential chain of dispersion exercises was carried out with this purpose. The overall idea is to harmonize models, making them run with the same forcing in a step-by-step procedure, in such a way that the main agent in producing discrepancy between models can be found. It was found that the main reason of discrepancies between models is due to the description of the hydrodynamics. However, once this has been sup-pressed, some variability between model outputs remains due to intrinsic differences between models (as numerical schemes). The numerical experiments were carried out for a perfectly conservative radionuclide and for ^{137}Cs (including water/sediment interactions). Model outputs for this radionuclide were also compared with measurements in water and sediments.

Keywords:

Fukushima Dai-ichi
Marine dispersion
Hydrodynamics
Sediments
Caesium-137

1. Introduction

Models play a major role in the cases of accidental releases of pollutants in order to obtain rapid assessment decision for countermeasures to minimize the potential impact on humans and the environment. The International Atomic Energy Agency (IAEA) has been organizing programmes of international model testing since the 1980s. The possible benefits of carrying out model validation and testing at an international level were recognized by the Swedish Radiation Protection Institute, which sponsored the Biospheric Model Validation Study (BIOMOVS) and BIOMOVS II programmes starting in 1985 (IAEA, 1996). BIOMOVS was the first international exercise aimed at the testing and validation of models for the prediction of radionuclide transfer through the environment to humans. The Chernobyl accident in 1986 created a renewed need for reliable assessments in many countries and provided an increased impetus for work in this area. It also created new data sets that could be put to use for model testing. As a consequence, the IAEA was prompted to start a programme on the Validation of Model Predictions (VAMP) in 1988, which concluded in 1996 (IAEA, 2000).

More recently, Environmental Modelling for Radiation Safety (EMRAS) program, running from 2003 to 2007, included a working group on *Testing of Models for Predicting the Behaviour of*

* Corresponding author.
E-mail address: rperianez@us.es (R. Periáñez).

Radionuclides in FreshWater Systems and Coastal Areas (IAEA, 2012; Monte et al., 2008). Five scenarios were studied in the frame of this project, among which there were two estuaries (Dnieper-Bug in Ukraine and Huelva in Spain). However, a properly marine environment was not considered. A specific working group for the aquatic environment was not included in EMRAS-II project.[1]

During the recent decade several significant developments indicate that a new international modelling exercise specifically carried out for the marine environment can achieve significant progress: new developments in modelling (complex 3-D hydrodynamic models, optimized coding allowing implementation of complex models, techniques involving various scales and deterministic/statistical approaches, ecological modelling, dynamic transfer models etc), improved knowledge of oceanographic and atmospheric drivers, increased database of generic and specific parameters, new knowledge of chemical form-specific biogeochemistry and the effect of environmental change (e.g. ocean acidification) on the fate of radionuclides in the marine environment.

The MODARIA[2] project, of the International Atomic Energy Agency (IAEA), was initiated to make progress in relation to the assessment of radioactive substances in the environment and its impact to man and biota. Working group 10 was dealing with modelling of marine dispersion and transfer of radionuclides accidentally released from land-based facilities. Different models developed in Member States were applied to the accidental releases and discharges from the Fukushima Dai-ichi accident in the Pacific and to the accidental fallout deposition on the Baltic Sea from the Chernobyl nuclear power plant disaster in 1986. The latter case caused a significant long-lasting contamination in this semi-enclosed sea area, primarily with ^{137}Cs and ^{134}Cs. Results of the Baltic Sea model comparison have been described in Periáñez et al. (2014). Fukushima results are presented in this paper.

After the 9.0 magnitude earthquake and resulting tsunami occurred on March 11th, 2011, significant amounts of radioactive material were released to the environment from Fukushima Dai-ichi nuclear power plant. Radionuclides released to the atmosphere were transported eastward by a strong jet stream and reached the coast of North America in four days (Takemura et al., 2011). A portion of these radionuclides was deposited on the Pacific Ocean surface by wet and dry deposition processes. In addition, water used to cool a damaged nuclear reactor leaked into the ocean (Kobayashi et al., 2013). Thus, two radionuclide sources into the ocean from Fukushima must be considered: direct discharge of contaminated water, over a period of several months with peak releases at the end of March and beginning April 2011, and deposition of radionuclides on the sea surface from the atmosphere.

The general large scale circulation in this region of the western Pacific Ocean is dominated by the interaction between the Kuroshio warm current (western boundary current in the north Pacific), which flows along the coast of Japan towards the north and curves to the central Pacific Ocean, and the Oyashio cold current from the north. These two current systems converge near the latitude of the coastal waters off Fukushima. Such convergence leads to the generation of unsteady eddies in the area and along the trans Pacific current system. It is also known that the Kuroshio current acts as a barrier, as described by Jayne et al. (2009), which prevents the migration of radionuclides released from Fukushima towards the south (they would not travel south beyond the latitude of Tokyo). Instead, they are transported eastwards towards the central Pacific (Kuroshio Extension).

A significant number of modelling studies on the dispersion of radionuclides released from Fukushima into the Pacific Ocean have been published in scientific literature. First studies were published soon after the accident. Thus, Kawamura et al. (2011) simulated the spreading of ^{131}I and ^{137}Cs using the Lagrangian model SEA-GEARN, developed at JAEA. Nakano and Povinec (2012) also used a Lagrangian code to simulate the dispersion of ^{137}Cs and ^{134}Cs in the world ocean up to 30 years after the accident. Annually averaged water circulation was used for this purpose. Tsumune et al. (2012) simulated ^{137}Cs dispersion using a high resolution (1 km) regional model during the first three months after the accident.

Another similar study is that of Estournel et al. (2012). They found that radionuclides stay close to the coastline for relatively long times and suggested the role of freshwater discharges from land in offshore dispersion events. Miyazawa et al. (2012), using as well an Eulerian dispersion model for ^{137}Cs, carried out some sensitivity studies to highlight the relevant role of winds in the shelf region.

Behrens et al. (2012) made 10 year long simulations of ^{137}Cs dispersion in the Pacific Ocean. Water circulation of the past 10 years was used for this purpose. They found that the initial current field is relevant for ^{137}Cs spreading in the first months after the accident, but this relevance fades in the long-term. Also, these authors found that the main tracer patch would reach the coast of North America after about 5–6 years, and that concentrations would be nearly homogeneous over the whole Pacific after some 10 years. Simulations finally indicate a fast mixing over the upper 500 m of the water column. Kawamura et al. (2014) also found that the radioactive caesium concentration due to the Fukushima disaster was efficiently diluted in the North Pacific 2.5 years after the accident. The meso-scale eddies in the Kuroshio Extension played an important role in diluting the radioactive patch. The ^{137}Cs concentrations in the surface, intermediate, and deep layers reduce to the pre-Fukushima values over the North Pacific some 2.5 years after the Fukushima accident. Similar conclusions were obtained by Rossi et al. (2013, 2014): the Fukushima plume is rapidly diluted within the Kuroshio system over a time-scale of a few months. Over the subsequent decades a significant amount of Fukushima-derived radionuclides will spread across the North-Pacific basin. The model estimates that a component of Fukushima ^{137}Cs will be injected into the interior ocean via subduction, before eventually returning to the surface by coastal upwelling along the west coast of North America.

Dietze and Kriest (2012), using a model, evaluated the residence time of ^{137}Cs in the shelf as 43 ± 16 days. Honda et al. (2012) studied the relevance of atmospheric deposition, finding that high ^{137}Cs concentrations detected in surface water north of 40°N one month after the accident must be attributed to atmospheric deposition.

More recently, Bailly du Bois et al. (2014) made a number of model sensitivity analysis and found that a tuning of the wind drag coefficient was required for a better reproduction of ^{137}Cs measurements. However, they used a direct release source term of 27 PBq (Bailly du Bois et al., 2012), which has been considered to be significantly biased high by Dietze and Kriest (2012).

Some other modelling studies have had the objective of determining the releases from Fukushima into the ocean, using inverse modelling. This has been done by Estournel et al. (2012) and Miyazawa et al. (2013), for instance.

All modelling studies mentioned above (which does not try to be an exhaustive list) present the common point that ^{137}Cs is treated as a tracer, a perfectly conservative radionuclide which does not interacts with sediments. The first models including ^{137}Cs contamination of bed sediments were described by Periáñez et al. (2012) and Min et al. (2013). In the first case a local study was carried out, covering only the coastal region of Japan. A larger

[1] http://www-ns.iaea.org/projects/emras/emras2/.

[2] Modelling and Data for Radiological Impact Assessments. Further information can be found here: http://www-ns.iaea.org/projects/modaria/default.asp?l=116.

domain was considered in the second paper. In both cases, calculated and measured ^{137}Cs concentrations in bed sediments were compared. Also, water-sediment interactions were described in a dynamic way in both studies. Choi et al. (2013) also include adsorption by bottom sediments. All these papers agree in the fact that a significant adsorption occurs in the first months after the accident, most of radionuclides staying on the seabed once they have been adsorbed. More recently, Maderich et al. (2014a) have used a box model (POSEIDON-R) to perform a radiological assessment of the accident in the period 2011–2040. This model includes not only adsorption to sediments, but also the transfer of radionuclides through the marine food web and subsequent doses to humans. A dynamic food-chain model was used.

Some models have finally been applied to other radionuclides, as ^{90}Sr (Periáñez et al., 2013a; Maderich et al., 2014b). The same coastal model commented above for ^{137}Cs was used in the first case. In the case of Maderich et al. work, POSEIDON-R model again was applied. Some preliminary simulations for plutonium were presented by Periáñez et al. (2013b).

Some exercises comparing model performances when applied to simulate the releases from Fukushima have been carried out, as for instance in Masumoto et al. (2012). These authors concluded that most of the discrepancies between the five participating models are due to the different calculated current fields in the coastal waters of Japan, off Fukushima, which lead to different radionuclide distributions. Differences in current fields are caused by the different models and model settings used by the research groups. However, a systematic assessment aimed at investigating the reasons of differences was not carried out.

The Science Council of Japan (SCJ, 2014) carried out a similar intercomparison study, with eleven models involved. Again, significant differences between models were found. Models were different in concept (Eulerian vs. Lagrangian), with different settings and even different source terms. Thus, it was concluded that a simple comparison is not straightforward and that detailed systematic comparison studies, such as ones that use the same radionuclide forcing with different models and/or the same model with different forcing scenarios, are required. As will be shown below, our objective consists of making such a systematic study.

The methodology followed in this model intercomparison is given in section 2, where the sequential chain of numerical experiments are described. Also, models participating are presented. Results of these experiments are described in section 3. In particular, comparisons of model outputs with measurements are given in section 3.4. The description of Fukushima releases are also included in this section.

2. Methods

Generally speaking, a marine dispersion model consists of two submodels. A hydrodynamic model will provide the water currents required to solve the advective transport of radionuclides. The dispersion model will use such currents to calculate transport including advection, mixing produced by turbulence and other processes like radioactive decay or interactions of dissolved radionuclides with suspended matter and bottom sediments. Also, the dispersion model may include a sediment transport module. Models will be compared in such a way that the reasons of the discrepancies between them can be assessed (i.e., if they are due to the hydrodynamic part or the dispersion part).

A sequential chain of dispersion exercises has been carried out to achieve such objective in the present work. They are summarized in Table 1. The overall idea is to harmonize models, making them run with the same forcing in a step-by-step procedure, in such a way that the main agent in producing discrepancy between models can be found. This type of intercomparison exercise has never been carried out before for marine dispersion models.

Table 1
Modelling exercises carried out for Fukushima scenario.

Exercise	Features	Source	Radionuclide
1	Own circulation and parameters	Hypothetical	Tracer
2	Same circulation, own parameters	Hypothetical	Tracer; ^{137}Cs
3	Same circulation and parameters	Hypothetical	Tracer; ^{137}Cs
4a	Same circulation and parameters	Realistic	^{137}Cs
4b	Own circulation and parameters	Realistic	^{137}Cs

Initially, dispersion exercises were carried out with a tracer (a perfectly conservative radionuclide). This way all parameters describing water-sediment interactions are avoided. Also, a constant source term, hypothetical, was used by all models. In exercise 1, each model used its own water circulation and set of parameters (like for instance horizontal and vertical diffusion coefficients). Then all models used the same hydrodynamic description in exercise 2. All parameters were homogenized in exercise 3. Finally, a realistic source term, both for direct releases into the ocean and atmospheric deposition on the sea surface, was used in exercise 4. This allows comparing model results with measurements of ^{137}Cs in water and sediments. This radionuclide was introduced from exercise 2 on. Exercise 3 was also carried out with and without suspended matter particles in the water column. A range of *model expertise* ^{137}Cs concentrations in water and sediments will be obtained from exercise 4 (exercise 4b). This range may be regarded as some kind of model uncertainty assessment. In this exercise each team will use its own model set-up and parameterization. In contrast, the common model configuration is used in exercise 4a.

The dispersion models which have been used in the Fukushima exercises described in this paper are listed in Table 2. More detailed descriptions are given in the corresponding appendixes and included references. Some of these models make their own calculation of hydrodynamics (IMMSP/KIOST with SELFE, Sisbahia models), while others import water circulation from operative ocean forecasting models (KAERI, JAEA and USEV models). These ocean circulation models are briefly described in Appendix A.

3. Results

3.1. Exercise 1

A very simple exercise was first carried out to evaluate the performances of models under simple conditions. Thus, a constant source of a perfectly conservative radionuclide was considered. The magnitude of the source was arbitrarily defined as 1.0×10^6 Bq/s of a long-lived radionuclide (radioactive decay can be neglected). The release was supposed to start on March 26, 2011, and time frame of calculations extends until May 30.

Each model was run using its own hydrodynamic description, as listed in Table 2, and set or required parameters. JAEA has applied

Table 2
Models applied to simulate Fukushima releases in the Pacific Ocean. The origin of water circulation is also given. Own means that it is calculated by the model; in other cases the name of the ocean forecasting model is given.

Model	Country	Circulation
IMMSP/KIOST	Ukraine/Rep. of Korea	Own (SELFE)
KAERI LORAS model	Rep. of Korea	NCOM and JCOPE2
JAEA SEA-GEARN model	Japan	Univ. of Kyoto
USEV-3D model	Spain	JCOPE2
Sisbahia model	Brasil	Own

two models, a finite difference (JAEA FDM) and a particle-tracking one (JAEA PT). KAERI has run the same model using circulation from two hydrodynamic models: JCOPE2 and NCOM. The output of the models are time series of tracer concentrations in the water surface at 3 points located in front of Fukushima NNP, at increasing distances from it. The locations of these points may be seen in the map in Fig. 1.

Results for point P2, which is the closest to Fukushima, are presented in Fig. 2 as an example. It may be seen that calculated concentrations expand over several orders of magnitude. A very noisy signal was produced by all models. This is attributed to the very rapidly changing water speeds and directions, as will be shown below. Point P1 is some tens of km offshore Fukushima. The arrival of the signal is similar for all models, although in the case of IMMSP/KIOST-E (IMMSP/KIOST will be abbreviated to I/K from here) there was a delay of about 20 days with respect to the others (results for P1 not shown).

In the case of point P3 (not shown), it is interesting to note that the arrival of the signal is similar for most models, about 40 days. Again, predictions expand over several orders of magnitude. Differences between Lagrangian particle-tracking (KAERI, JAEA PT) and Eulerian techniques (JAEA FDM, I/K-E) are clearly apparent in this point. Finite differences introduce artificial (numerical) diffusion. Thus, once the signal has arrived to the location of interest, a continuous line is obtained for the time series of concentrations. However, numerical diffusion is not introduced by particle-tracking methods. These models give a concentration above zero at a given location only if there is at least one particle there. Consequently, periods with zero concentration may alternate with periods during which some finite concentration is computed.

A better agreement between the outputs of dispersion models should be expected if the same water circulation is used by all of them. This would be exercise 2. A previous step must be defining which is the most appropriate hydrodynamic model to be used. A quantitative comparison of hydrodynamic model outputs was carried out with this purpose.

3.2. Exercise 2

Given the significant discrepancies in model results, even in the very simple case of a perfectly conservative radionuclide and a constant release, that have arisen from dispersion exercise number 1, the outputs of the hydrodynamic models which have been used to calculate dispersion were compared. The final objective consisted of selecting the most adequate hydrodynamic model to be used in all dispersion models. Thus, all dispersion calculations would be carried out with the same hydrodynamic forcing and, consequently, this source of discrepancy would be removed.

As an example, water currents in the sea surface for March 26th calculated by some hydrodynamic models are presented in Fig. 3. It is clear that the overall picture provided by all models is similar: the Kuroshio current, flowing to the northeast is clearly visible. But differences can also be appreciated, with meanders and gyres which are produced by some models but not by others.

Time series of water current magnitude and direction calculated by the models are presented in Fig. 4 for P2 at the sea surface. This is the closest point to Fukushima plant. The order of magnitude of the calculated currents is the same, but there are significant differences between models if the current magnitude and its direction are compared for a given instant of time. Consequently, it is not surprising that there are significant differences in calculated radionuclide concentrations between the models, even in the simple case of exercise 1. The different water velocities and directions in the vicinity of the release point lead to significantly different dispersion paths in the initial stages, which in turn implies that extremely different radionuclide concentrations are produced by the models.

An objective comparison between calculated sea surface temperature (SST) fields and satellite observations was carried out to evaluate closeness between hydrodynamic model fields, and then assess which model may provide the most realistic picture of circulation. SST fields were used since they can be more easily handled than current fields (it is a scalar instead of a vectorial field). Also, SST can be easily obtained from satellite observations. Finally, SST is essential in determining baroclinic circulation. Thus, a good SST

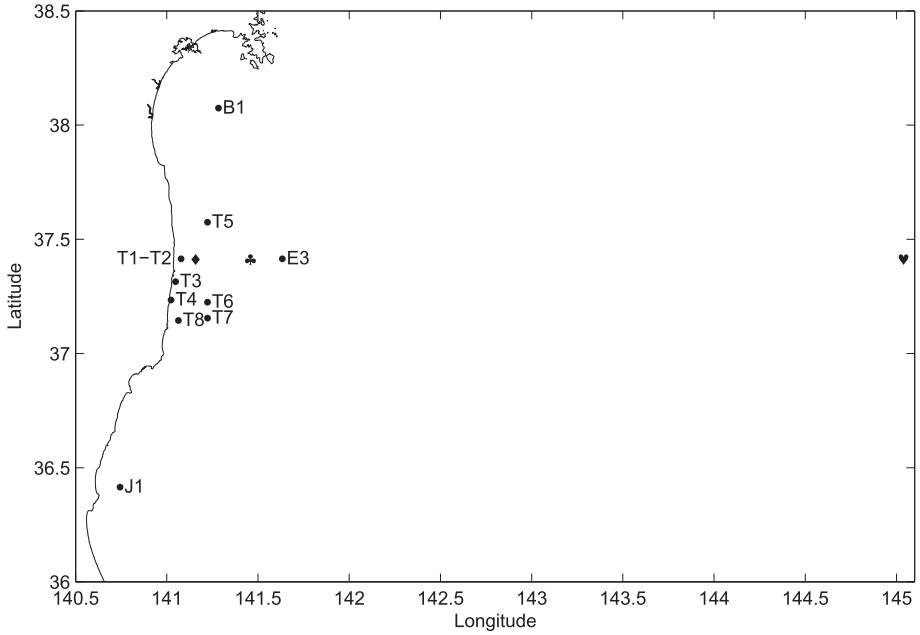

Fig. 1. Location of sampling points where calculated ^{137}Cs concentrations in surface water have been compared with measurements. Filled ◊ is P2, ♣ is P1 and filled ♡ is P3.

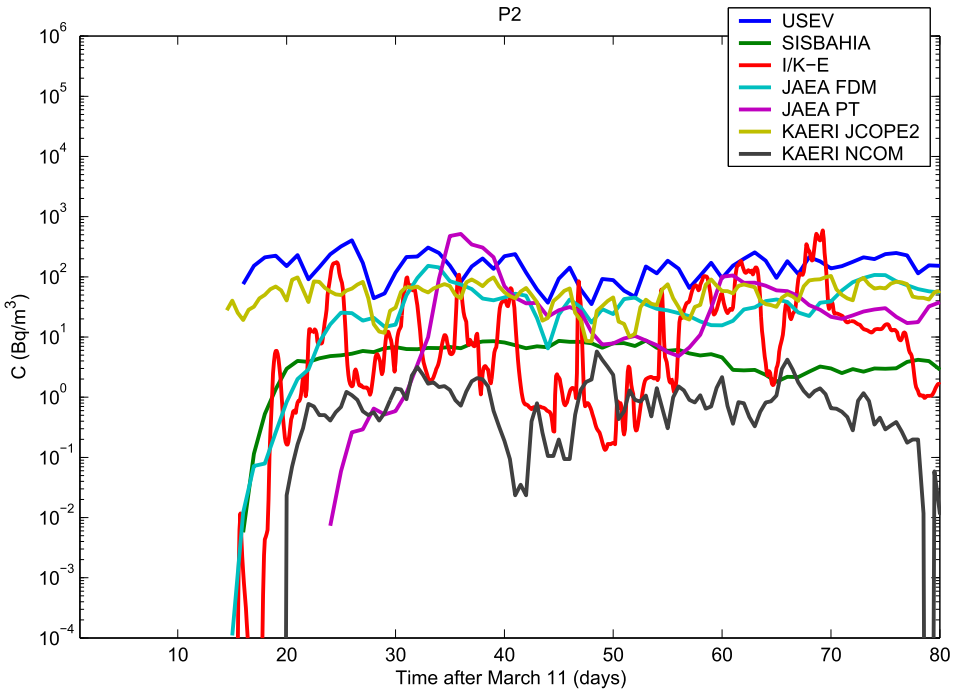

Fig. 2. Calculated concentrations (Bq/m^3) at the sea surface in point P2 for exercise 1. I/K-E means the IMMSP/KIOST model in Eulerian mode.

description is required to have a realistic representation of circulation.

The SST gridded fields averaged for first week of April 2011 were provided by 7 regional models (Appendix A): HYCOM, Univ. of Kyoto, JCOPE2, MARS, NCOM, SELFE and SYMPHONIE.

The computed fields were interpolated on the same regular grid with 200 × 200 cells for a domain extending 140.5–144°E in longitude and 35.5–38°N in latitude. The same coastal line mask was applied to all data. The daily satellite SST fields were averaged, then remaining gaps in observations were filled by linear interpolation from surrounding areas. The field was smoothed and interpolated into the same grid as computation data.

A simple method of classification [etalon-field method (Martazinova, 2005)] was applied. Details are not given, but the final conclusion was that JCOPE2 circulation is a reasonable selection to carry out the following dispersion exercises, in which all models used the same hydrodynamics.

As in the case of exercise 1, the magnitude of the source was 1.0×10^6 Bq/s of a long-lived radionuclide (radioactive decay can be neglected). The release was supposed to start on March 26, 2011, and time frame of calculations extended until May 30.

This exercise was carried out for two cases: a tracer (perfectly conservative radionuclide) and ^{137}Cs (including interactions with bed sediments). Thus, the first case is exactly like exercise 1, but using the same water circulation by all models. Other model settings were left as originally defined. Each model also used its own configuration and parameters to define water-sediment interactions.

Mean daily three-dimensional water currents computed by JCOPE2 were distributed to all participants and models were appropriately modified to import such data. In the case of the tracer, model end-points were exactly the same as in exercise 1: time series of tracer concentrations at the water surface in points P1, P2 and P3. Time series at the same points were provided for ^{137}Cs, but for surface water, bottom water (in the deepest layer, in contact with the seabed) and sediments.

3.2.1. Tracer dispersion

Results for the tracer dispersion exercise are presented in Fig. 5. It may be observed that, generally speaking, the agreement between models has been significantly improved. The shapes of the signals are much more similar than in exercise 1. On the other hand, results are within one order of magnitude.

Although at some times and locations some significant differences between models still remain (see for instance point P1, some 30 days after March 11), most of the variability has been removed by the use of the same water circulation. This results the main factor of variability when the transport of a tracer is simulated.

3.2.2. ^{137}Cs dispersion

In order to simplify the problem, it was considered that bed sediments were uniform over all the model domain and composed entirely of fine material (clays) with mean size 10 μm. A uniform porosity of 0.6 was assumed and, finally, the thickness of the sediment (which interacts with water) was set to 10 cm. With this homogenization it is assured that differences between model outputs are due to intrinsic factors of the models, but not to input data. It must be noted that now the objective is to make comparisons between models, not to compare model results with measurement. Thus, hypothetical (but realistic) values for some parameters may be used. Time series of ^{137}Cs concentrations for surface water, bottom water (deepest water layer, in contact with the seabed) were provided at points P1 to P3, as commented above.

Results of this exercise are presented in Fig. 6 for P2 as an example. In the case of surface water, results from all models are similar, like in the tracer exercise. The reason is that surface water is scarcely sensitive to the presence of the bed sediment, specially when water depth increases. The arrival to the signal to point P3 (not shown) produced by KAERI and JAEA models is in very good agreement.

In the case of bottom water, very low concentrations were calculated by all models in point P1 (not shown). At P2 (Fig. 6), close to Fukushima release point, higher concentrations were calculated

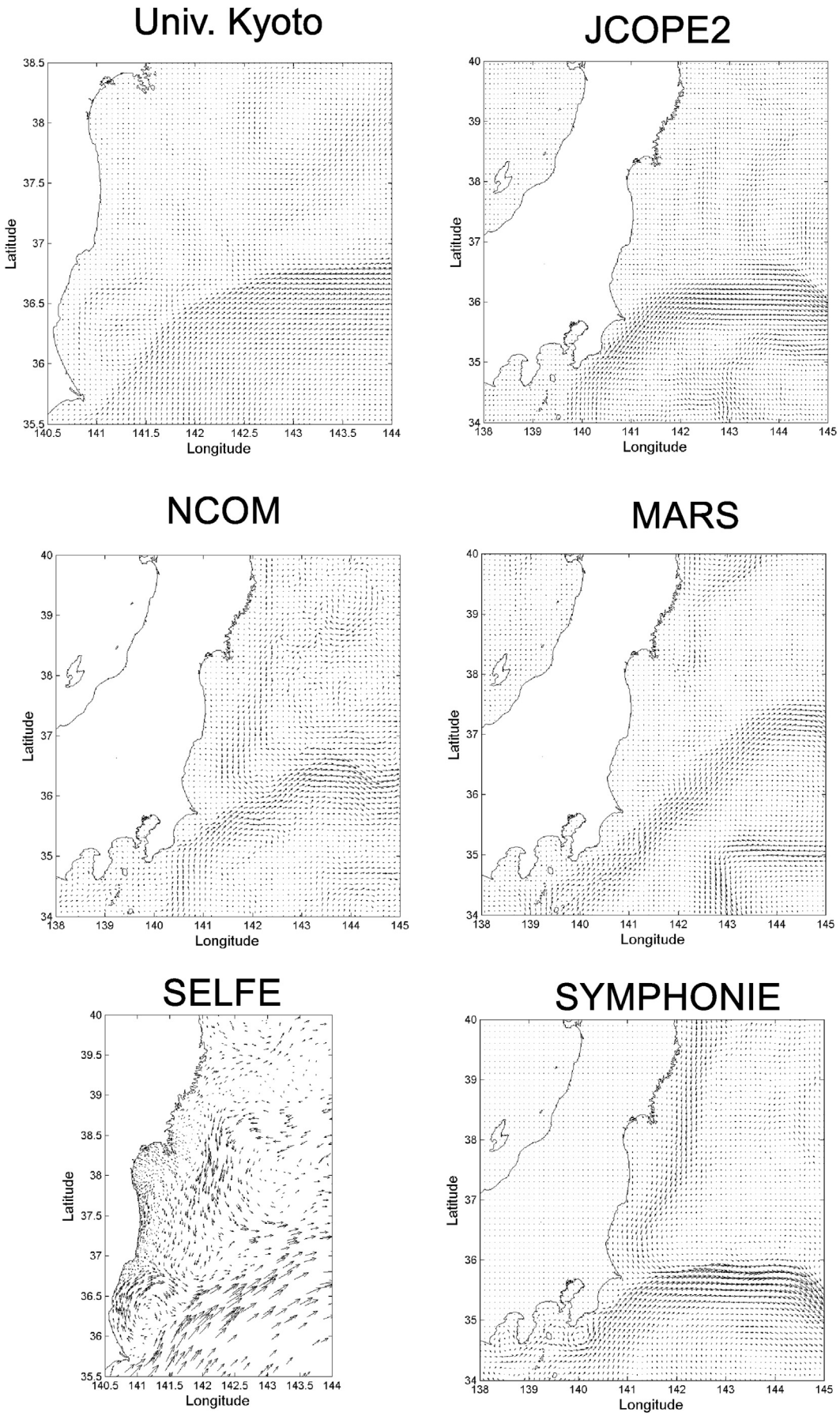

Fig. 3. Water currents in the sea surface for March 26th calculated by some hydrodynamic models.

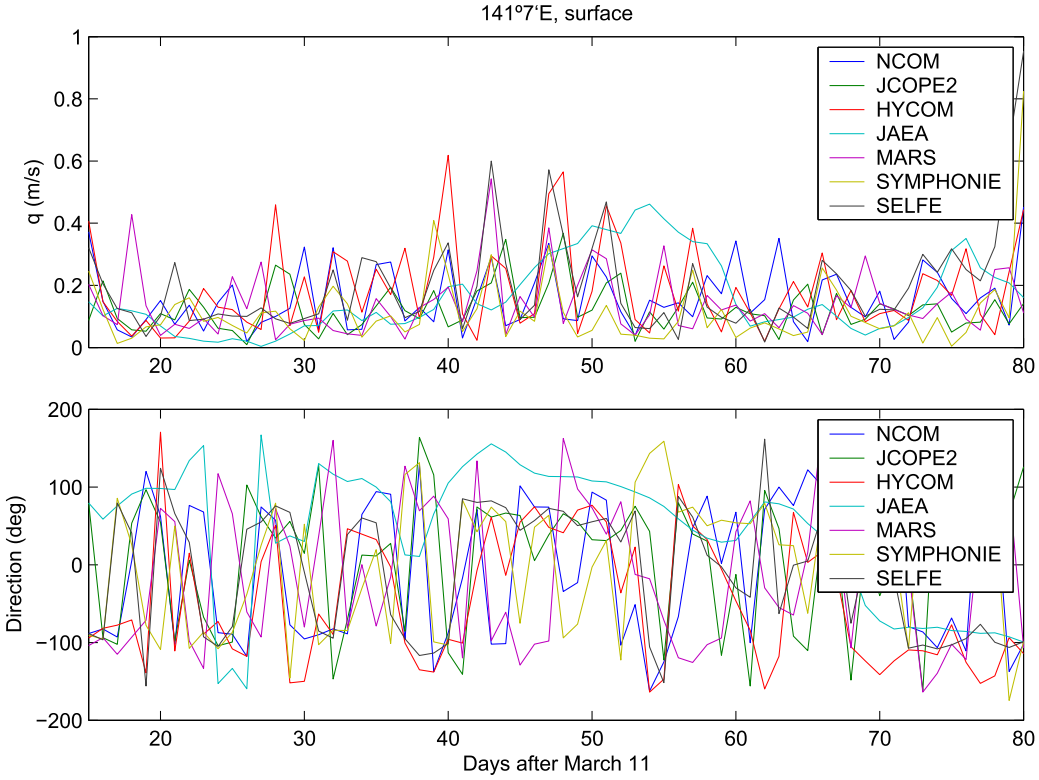

Fig. 4. Time series of surface current magnitude and direction calculated by the different hydrodynamic models in point P2. Current direction is measured in degrees counter-clockwise from east.

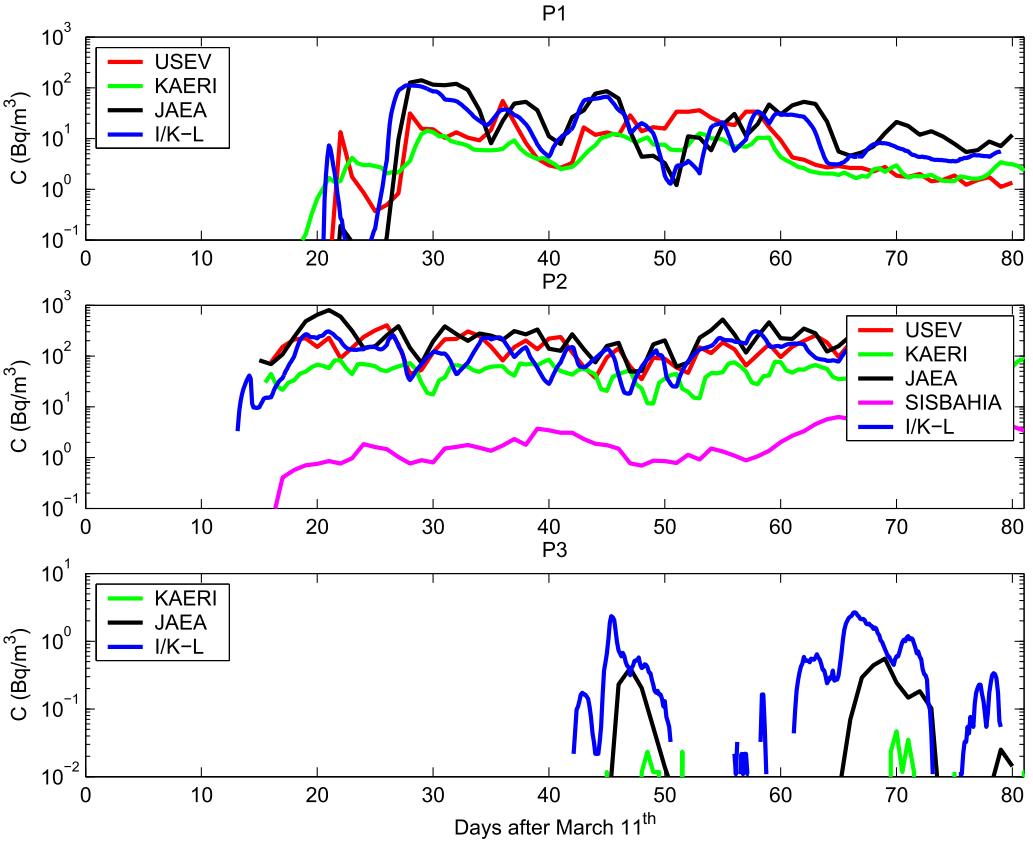

Fig. 5. Time series of radionuclide concentrations at points P1, P2 and P3 for the tracer exercise number 2. I/K-L means the IMMSP/KIOST model in Lagrangian mode.

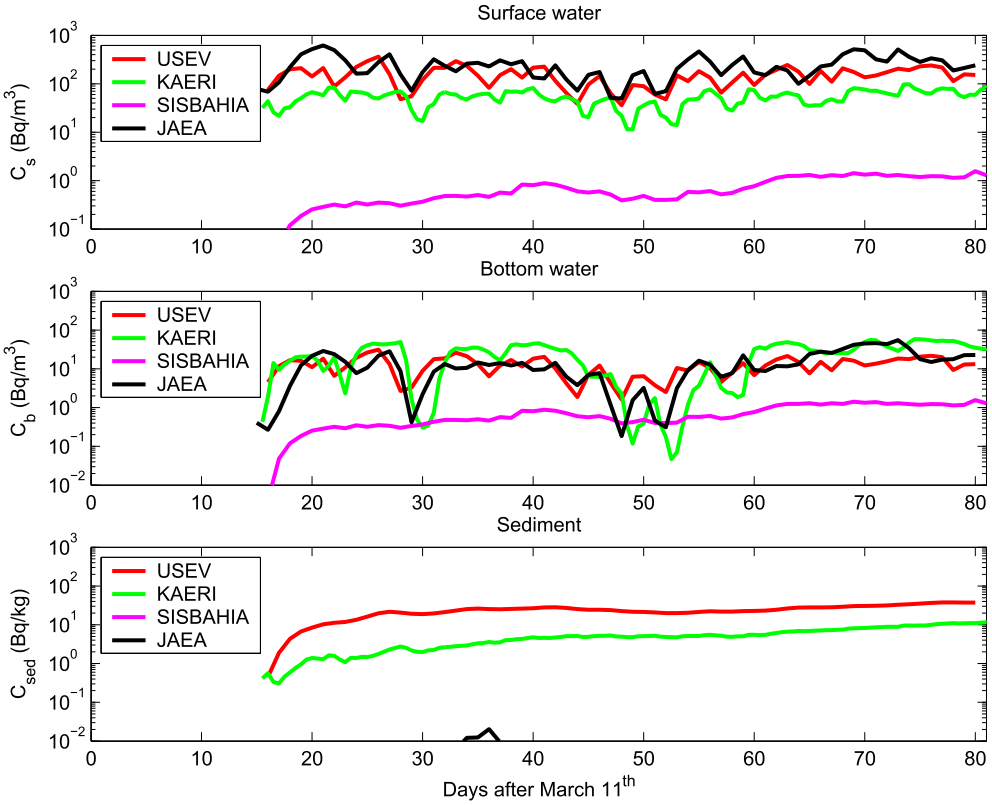

Fig. 6. Time series of radionuclide concentrations (^{137}Cs) at point P2 for surface water, bottom water and sediment. Exercise 2.

in bottom water. The signal was similar for most models.

Most of the variability between models is now obtained for the bed sediment. In point P2 (Fig. 6), for instance, results expand over several orders of magnitude. In general, JAEA model tends to produce lower concentrations in sediments than the other models.

As a conclusion from this exercise, it can be stated that when the dispersion of a tracer is simulated, a significant part of the variability between models is due to the water circulation. Model agreement increases if the same circulation data is applied by all models.

In the case of ^{137}Cs, including water sediment interactions, there were significant differences between models, with calculated concentrations in the seabed expanding over several orders of magnitude. Nevertheless, agreement between models in the dissolved phase was similar to the tracer case. Each model used its own description for water/sediment interactions, as well as its own set of parameters for describing such process. The next obvious stage is to homogenize the description of water/sediment interactions, using equivalent parameters in all models.

3.3. Exercise 3

This exercise was designed as in the previous cases. A constant release of 1.0×10^6 Bq/s of a long-lived radionuclide (radioactive decay can be neglected) was used. The release was supposed to start on March 26, 2011, and time frame of calculations extended until May 30. However, exactly the same bathymetric file, which has been distributed to all groups, was used by all models. In addition, the same diffusion coefficients were used. Constant and uniform reasonable values were defined. The purpose of using constant and uniform values was to remove additional variability between models which would be introduced if, for instance, a Smagorinsky's scheme was used to compute the horizontal diffusion coefficient and/or any turbulence model was applied to calculate the vertical diffusivity.

In addition, the same parameters were used to simulate uptake/release with sediments. Models may use a distribution coefficient or, alternatively, kinetic transfer coefficients. Values for the two options were defined. The equilibrium distribution coefficient is: 2.0 m^3/kg. This is the mean value recognized by IAEA (2004) for open ocean waters and is also in agreement with measurements off Fukushima (Honda et al., 2012). The rate describing release from sediments is: $k_2 = 1.16 \times 10^{-5}$ s^{-1}. The kinetic rate describing uptake (k_1) was derived from k_2 and the distribution coefficient as usual (Periáñez, 2005).

3.3.1. Tracer dispersion

Results for the tracer exercise are summarized in Fig. 7. Results are within the same order of magnitude for all models in points P1 and P2 (note that now a linear scale has been used for the y axis instead of a logarithmic one as before). Thus, in general, the use of the same bathymetry and diffusion coefficients has slightly improved the agreement between models. Nevertheless, as it could be seen from exercises 1 and 2, the main factor in producing model discrepancies is water circulation. In other words, the agreement improvement was higher from exercise 1 to 2 than from exercise 2 to 3.

In the case of P3, results were similar to those of exercise 2. The agreement between models was relatively good for both the arrival of the signal and the calculated concentrations.

3.3.2. ^{137}Cs dispersion

Calculated time series for ^{137}Cs at point P2 are presented in Fig. 8 as an example. It may be seen that the use of the same parameters

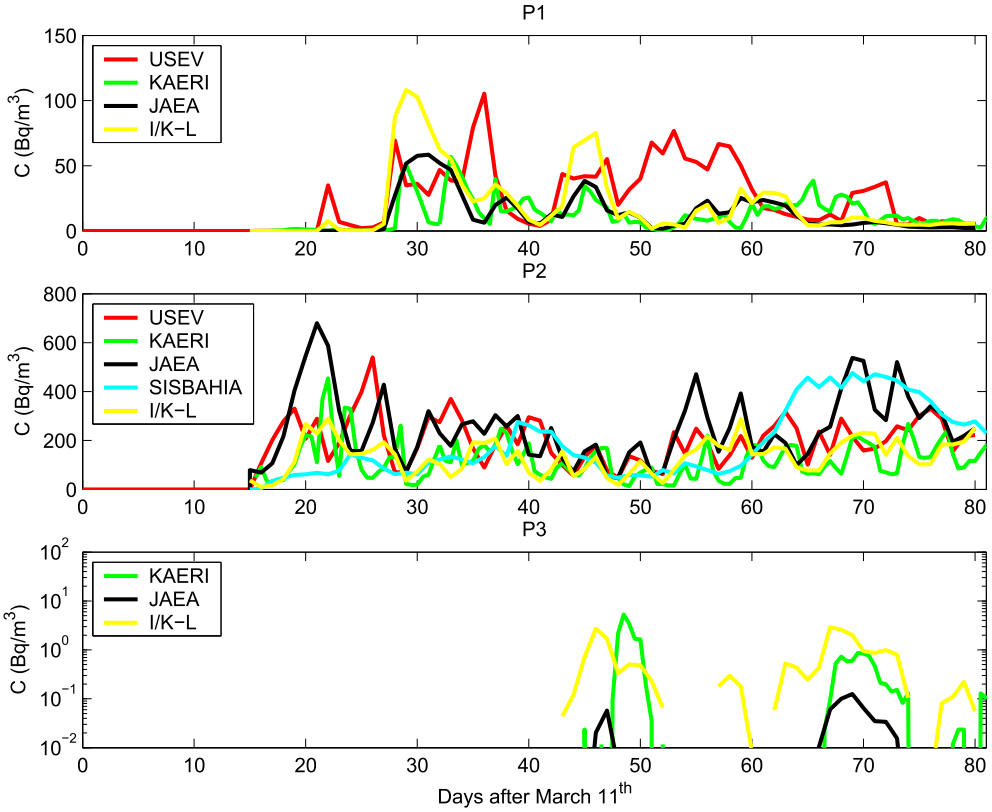

Fig. 7. Time series of radionuclide concentrations at points P1, P2 and P3 for the tracer exercise number 3.

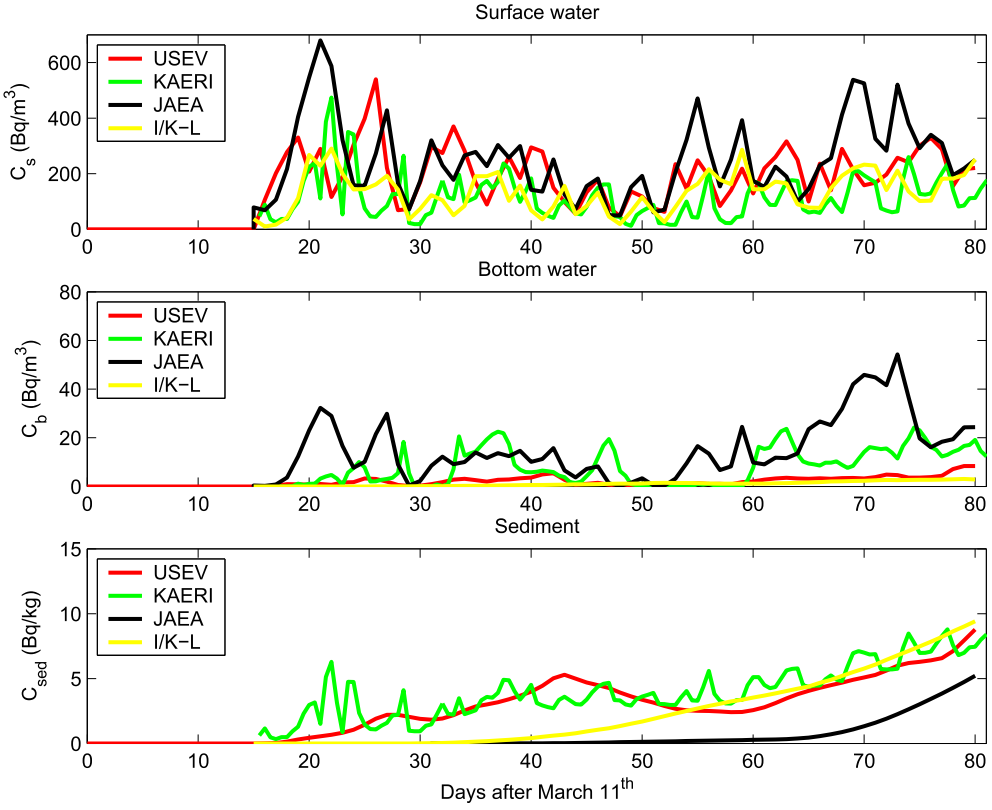

Fig. 8. Time series of radionuclide concentrations (^{137}Cs) at point P2 for surface water, bottom water and sediment. Exercise 3 without SPM.

has improved model agreement. Model results were, in general, within the same order of magnitude (note that logarithm scale is not been used). In the case of bed sediments, JAEA model produced lower concentrations than KAERI, I/K-L and USEV models at P1 (not shown), which were more similar. In the case of P2, results from these four models gave a good agreement.

In the case of P3 (not shown), the new values defined for the diffusion coefficients led to a very weak signal. ^{137}Cs did not seem to reach neither the bottom water nor the bed sediment.

This exercise was repeated with a constant and uniform suspended matter concentration (SPM) in the water column equal to 5 mg/l. Essentially, results (not shown) were the same as in the exercise without SPM. This is not surprising given the relatively low affinity of ^{137}Cs to be fixed to solid particles. This affinity is quantified by the partition coefficient, which is defined as (Duursma and Carroll, 1996; Periáñez, 2005):

$$PC = \frac{1}{1 + k_d \cdot SPM} \quad (1)$$

where SPM is the suspended particulate matter concentration and k_d the corresponding distribution coefficient of the radionuclide. This coefficient gives the fraction of radionuclides remaining dissolved, under equilibrium conditions, for a given k_d value and suspended matter concentration. For $SPM = 5$ mg/L and $k_d = 2 \times 10^3$ L/kg, which were the values fixed for the exercise, it was obtained that $PC = 0.99$, indicating that most of ^{137}Cs remains in solution (99%), not being significantly adsorbed on suspended particles. Hence, the contamination of the bed sediment caused by deposition processes was negligible as well. Contamination of the bed sediment was mainly produced by direct adsorption of dissolved radionuclides present in the bottom water. Actually, the water-sediment interface may be considered as a high suspended matter environment (Li et al., 1984). Thus, the corresponding PC value would be significantly higher here and a significant fraction of ^{137}Cs would be adsorbed on the seabed.

Maps showing the computed distribution of ^{137}Cs in bed sediments are presented in Fig. 9, for JAEA and KAERI models as examples. Generally speaking, it may be seen that the behaviour of the radionuclide patch was very similar. For the dissolved phase (not shown), there was a remarkable agreement between both models. Essentially the same radionuclide patches were produced in surface water by these models.

3.4. Comparisons with field data

3.4.1. Source term

In order to compare model predictions with radionuclide concentration measurements in the marine environment off Fukushima, a realistic ^{137}Cs source term must be used. Radionuclides were introduced in the Pacific Ocean both from deposition on the sea surface of radionuclides previously released to the atmosphere and because of direct discharge and leakages of contaminated water into the sea. The reconstructions of source terms are described below.

3.4.1.1. Atmospheric deposition. Two atmospheric dispersion models were applied to simulate the dispersion of radionuclides released to the atmosphere and evaluate the subsequent deposition on the sea surface. These models were developed by KAERI and JAEA. The output from both models was compared and the ensemble average from both was taken as the best possible estimate of deposition.

The main characteristics of the applied atmospheric dispersion models are presented in Table 3. LADAS (Long-range Accident Dose Assessment system) was developed by Korea Atomic Energy Research Institute (Suh et al., 2006, 2009). WSPEEDI-II (Worldwide Version of System for Prediction of Environmental Emergency Dose Information) was used by the Japan Atomic Energy Agency (Terada et al., 2012). Both are particle tracking dispersion models.

A comparison (not shown) of the time series of calculated deposition at points P1, P2 and P3 gave, in general, a reasonable agreement between both models, which produced essentially the same deposition patterns. Main differences appeared at point P2, and are due to the use of different meteorological data, specially precipitation data required to simulate wet deposition. Thus, ensemble average values of deposition from both models, calculated over the whole domain of JCOPE2 circulation, was used for the realistic Fukushima simulations. Integrated deposition over time intervals of three hours were used.

As an example, ensemble average depositions over the domain for three time intervals during March are presented in Fig. 10. It may be seen that soon after the tsunami the atmospheric plume was directed to the north-east. On March 16th, a significant deposition occurred inland. Three days later, the plume curved to the south, although deposition was reduced by one order of magnitude.

3.4.1.2. Direct releases and leakages. The source term of ^{137}Cs released directly into the ocean from the Fukushima Daiichi NPP was estimated as described below. Full details are given in Kobayashi et al. (2013). Monitoring data from the web site of Tokyo Electric Power Company (TEPCO), regarding the area near the northern and southern discharge channels of the Fukushima Daiichi NPP, were used (TEPCO, 2011a) for this purpose.

The release point was determined to be the middle point along the coast between the northern discharge channel and the southern discharge channel of the Fukushima Daiichi NPP. It was assumed that the direct release into the ocean started on March 26. This was indicated by the analysis of the ^{131}I/^{137}Cs activity ratios (Tsumune et al., 2012) in ocean water. Discharges were assumed to continue until June 30. The amount of ^{137}Cs released directly into the ocean was estimated based on their concentrations at the northern and southern discharge channels of the Fukushima Daiichi NPP, which were monitored almost twice a day. First, the daily concentrations were averaged, and then the amount of ^{137}Cs at the sea surface within a volume of 1.5 km $\times$ 1.5 km $\times$ 1 m was calculated assuming that ^{137}Cs with averaged concentrations exists in the volume, because the distance between the northern and southern discharge channels is about 1.5 km. Finally, the calculated amounts were adjusted by multiplying the constant (7.5) obtained from a comparison of the total released amount of ^{137}Cs during 120 h from April 1 to April 6 with the values reported by TEPCO, which states that the total released amount of ^{137}Cs during this period was 0.94 PBq.

Fig. 11 shows the resulting temporal variation of the released amount of ^{137}Cs to be used in the simulations. This source term estimation led to a total ^{137}Cs release of 3.5 PBq from March 26th to June 30.

3.4.2. ^{137}Cs dispersion

The time frame of calculations extended from March 12 until June 30. Time series of calculated ^{137}Cs concentrations in surface water were provided by models for the points shown in Fig. 1, for which time series of measured concentrations were obtained by TEPCO (T1 to T8). These measurements were reported in regular press releases (TEPCO, 2011b). Three additional points sampled by Oikawa et al. (2013) were added to compare model results with measurements taken at larger distances from Fukushima.

A comparison of model results with ^{137}Cs measurements in

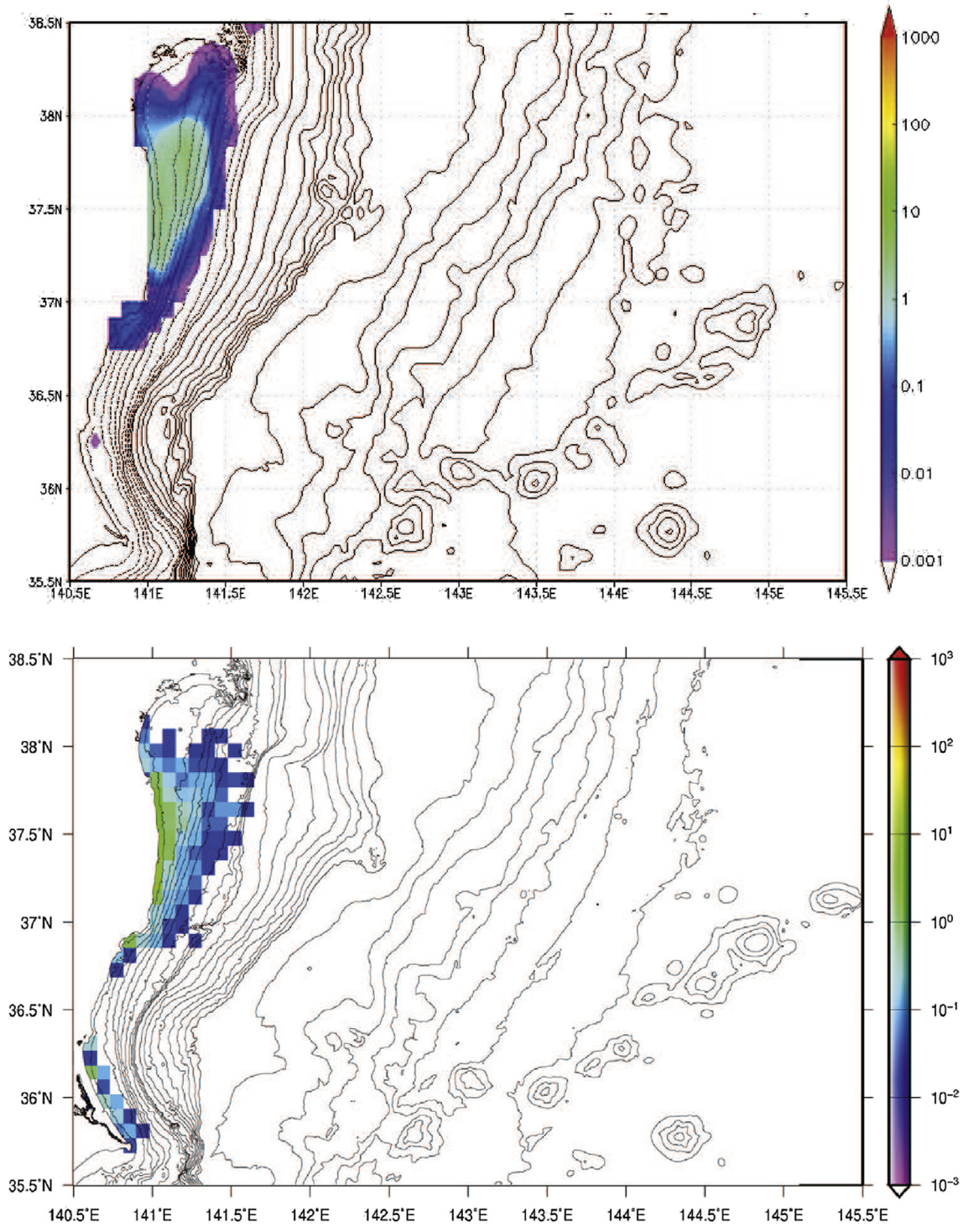

Fig. 9. Calculated ^{137}Cs distribution at bed sediments (Bq/kg) by JAEA (top) and KAERI (bottom) models for the ^{137}Cs exercise with SPM in the water column. Results correspond to May 30th, 2011.

surface water for exercise 4a (JCOPE2 circulation and same parameters) may be seen in Figs. 12 and 13 for points T1-T8 and the three additional points at far distances from Fukushima, respectively. The general structure of the time series was very similar in all models, since the same water circulation was used. There was also an acceptable agreement with measured concentrations. At large distances from Fukushima, all models agreed in producing concentrations below 10 Bq/L (except in E3). Additionally, peaks were generated at approximately the same time periods, except in B1, where a more noisy signal was produced by some models.

Results for exercise 4b are presented in Figs. 13 and 14. The decrease in concentrations which was produced by models around day 50 in exercise 4a at some points (with JCOPE2 circulation) is now not observed in JAEA model (see for instance T4), which reproduced very well the measured concentrations. This models used water circulation from the University of Kyoto hydrodynamic

Table 3
Main characteristics of atmospheric dispersion models. JST and KST are, respectively, Japan and Korea standard times. K_h and K_v are the horizontal and vertical diffusion coefficients and *Sc* means scavenging (s^{-1}). ♯Mellor and Yamada (1982).

	WSPEEDI-II	LADAS
Meteorological data	Japan meteorological Agency and MM5	Korea meteorological Administration
Domain	34-40°N, 138–145°E	34-40°N, 138–145°E
Horizontal resolution	6 km × 6 km	12 km × 12 km
Simulation period	2011.3.11, 23 h - 2011.5.30, 17 h (JST)	2011.3.12, 5 h - 2011.5.31, 0 h (KST)
^{137}Cs source	Terada et al. (2012)	Terada et al. (2012)
Release height	20 m, 120 m	20 m
K_h	Gifford (1982)	2.5×10^4 m^2/s
K_v	Mellor-Yamada♯ level 2.5	1.0 m^2/s
Dry deposition velocity	0.001 m/s 0.005 m/s on forests	0.001 m/s
Wet deposition scheme	$Sc = 5.0 \times 10^{-5} I^{0.8}$ *I*: precipitation (mm/h)	$Sc = 5.0 \times 10^{-5} I^{0.8}$ *I*: precipitation (mm/h)
Output interval	3 h	3 h

model, which has a higher spatial resolution in the area of Fukushima than JCOPE2. This higher resolution may be leading to a more accurate circulation in the area and a less noisy concentration time series. Generally speaking, except in the case of JAEA, models tended to underestimate dissolved ^{137}Cs concentrations.

Model results for seabed sediment ^{137}Cs concentrations were also compared with measurements. Results for exercise 4a are presented in Fig. 15. Here, the computed concentrations at the end of the simulation period (June 30) are drawn together with TEPCO measurements. Given that the same water circulation was used in all models, the resulting ^{137}Cs distributions in sediments resulted similar, with the highest concentrations in the area of Fukushima and some extension towards the south and northeast. There is consensus in the fact that most of the ^{137}Cs remains in a band along the coast and model results generally agree by order of magnitude with measurements.

In the case of exercise 4b, results for the bed sediment are presented in Fig. 16. The use of different water circulation led to different distributions of ^{137}Cs in sediments. It is particularly interesting to observe that the University of Kyoto circulation (in

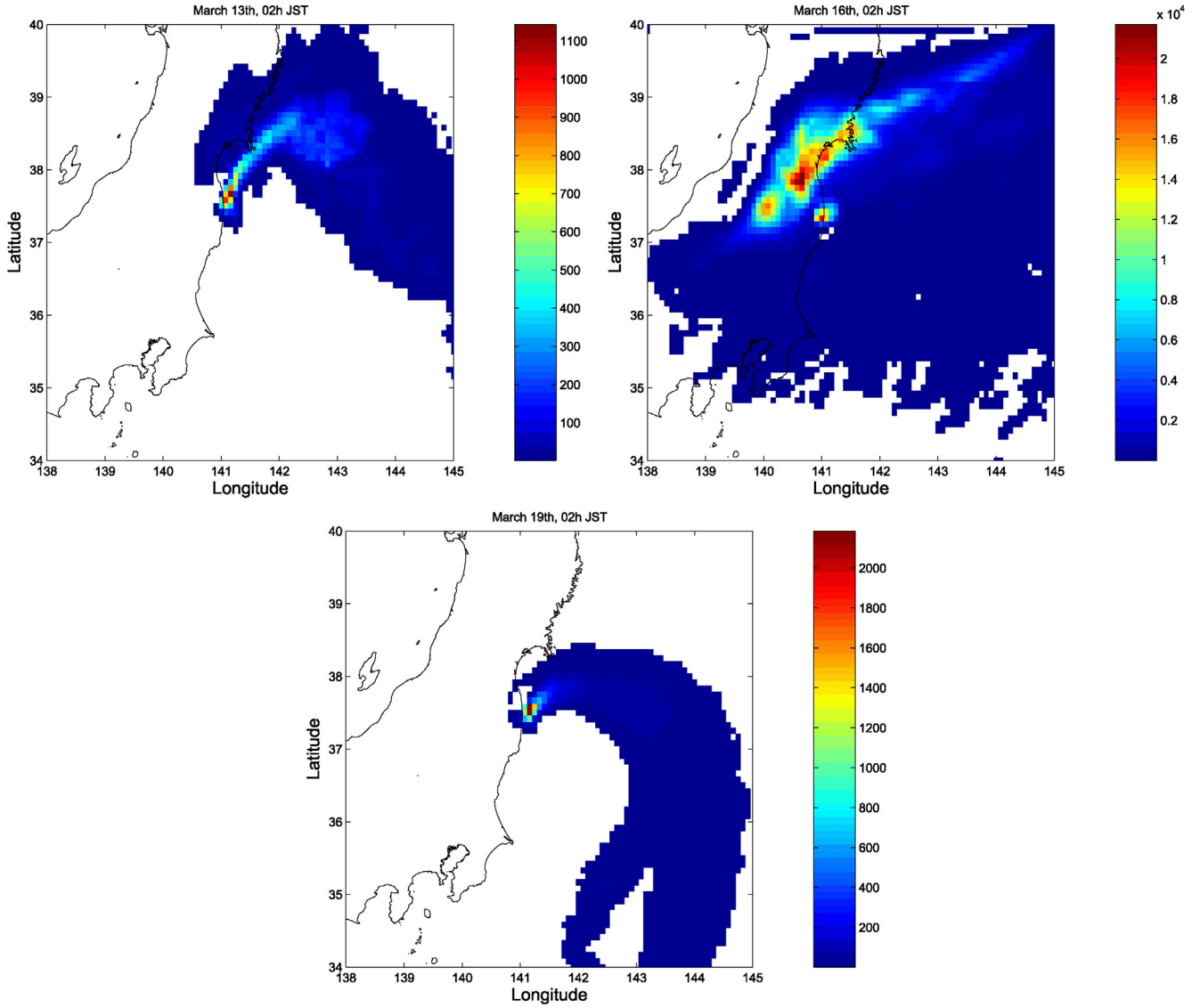

Fig. 10. Examples of calculated ^{137}Cs depositions (Bq/m^2) at three dates over the JCOPE2 domain. The ensemble average between both models is presented. Data correspond to integrated depositions over a three hour time interval. Japanese Standard Time (JST) is 9 h ahead of UTC.

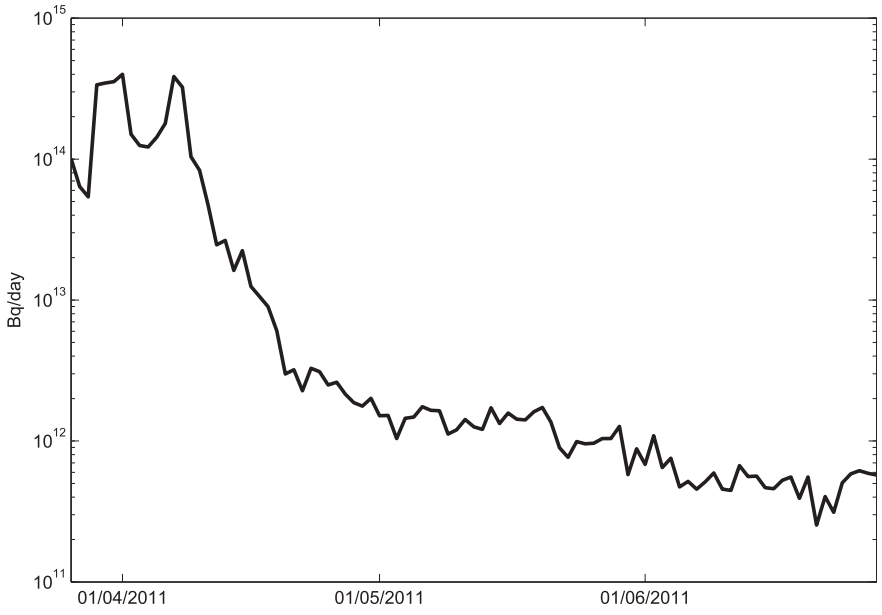

Fig. 11. ^{137}Cs daily direct releases to the Pacific Ocean from March 26 to June 30.

JAEA model) led to a very narrow contaminated band along the coast and in the Bay of Sendai. There was not any extension of ^{137}Cs north of 38.5° latitude, as found in measurements. However, dissolved concentrations calculated with this model were in the best agreement with measurements. Thus, JAEA model is performing better than the others when calculating surface dissolved concentrations, but worse than the others for the bed sediment. This cannot be attributed to the water/sediment interaction description, since in the case of exercise 4a (Fig. 15) output of this model was similar to the others. Instead, it seems that the University of Kyoto circulation model does not accurately reproduce deep circulation. In this sense, it has already been pointed out (Monte et al., 2006) that models may perform differently depending on the target variable. For instance, one model may predict radionuclide concentrations in bed sediments in good agreement with measurements, but it may provide not so good results for the water column. For another model, the situation may be the opposite.

The differences between Eulerian (I/K-E and USEV) and Lagrangian (JAEA and KAERI) models may be clearly appreciated from the maps of sediment concentrations (Figs. 15 and 16). Eulerian models introduce artificial (numerical) diffusion which leads to smother concentrations maps, with ^{137}Cs present over all the domain. However, the differences between the I/K model in Lagrangian and Eulerian modes were relatively small in Fig. 16.

Some comments should be given with respect to the possible contamination of model results by the previous knowledge of measured data. While exercises 1 to 3 were completely blind model tests, this is not entirely true for exercise 4b. In the case of I/K model, the desorption rate from the sediment was fitted to reproduce the measured inventory (Black and Buesseler, 2014) in the bed sediment. However, model results can be considered as blind for the dissolved concentrations. Exactly the same occurred in the case of USEV model. KAERI model was slightly modified with respect to exercises 1–3 to obtain a better agreement with observations. This modification consisted of making the release in a single point instead of into an Eulerian grid cell. Also, it was found that the best agreement with observations was obtained with parameters defined in exercise 3. Consequently, results for KAERI model exercises 4a and 4b were the same. KAERI model results cannot be considered blind. Finally, JAEA model application has been a blind exercise for both water and sediments.

In spite of some contamination of model results by knowledge of data, model results were in general consistent between them and with observations. The range of computed values for a given target variable may be regarded as an estimation of model uncertainty. Nevertheless, it seems that in general ^{137}Cs concentrations in surface water tend to be underestimated, while a good representation of sediments was generally obtained.

4. Summary and conclusions

A sequence of numerical exercises was carried out in which a progressive harmonization of models (understood as using the same forcing and parameterizations) was performed.

Initially, an exercise concerning a constant release of a perfectly conservative radionuclide (a tracer) was carried out. In these calculations, each modelling team used its own configuration for the model (set-up, parameters) and water circulation in the Pacific Ocean (this may be calculated by the model itself in some cases or imported from operative ocean forecasting systems in others).

Results from this exercise presented a significant variability (several orders of magnitude) between model outputs, even in a point very close to Fukushima outlet.

This variability in model results can be first attributed to the different descriptions of hydrodynamics in each model. Actually, water currents are the dominant factor in determining tracer dispersion in the marine environment. Consequently, model variability could be reduced if all the dispersion models were run with exactly the same description of water circulation for the period of interest.

To perform this task, the hydrodynamic description to be used by the participating teams must be selected. A comparison of the hydrodynamics (calculated or imported) used by each model was carried out. The overall patterns of currents provided by the models were similar, showing the same general features (as the Kuroshio current). However, a comparison of time series of water current magnitude and direction at a given point showed a strong variability in the signals produced by the models. Thus, it is not

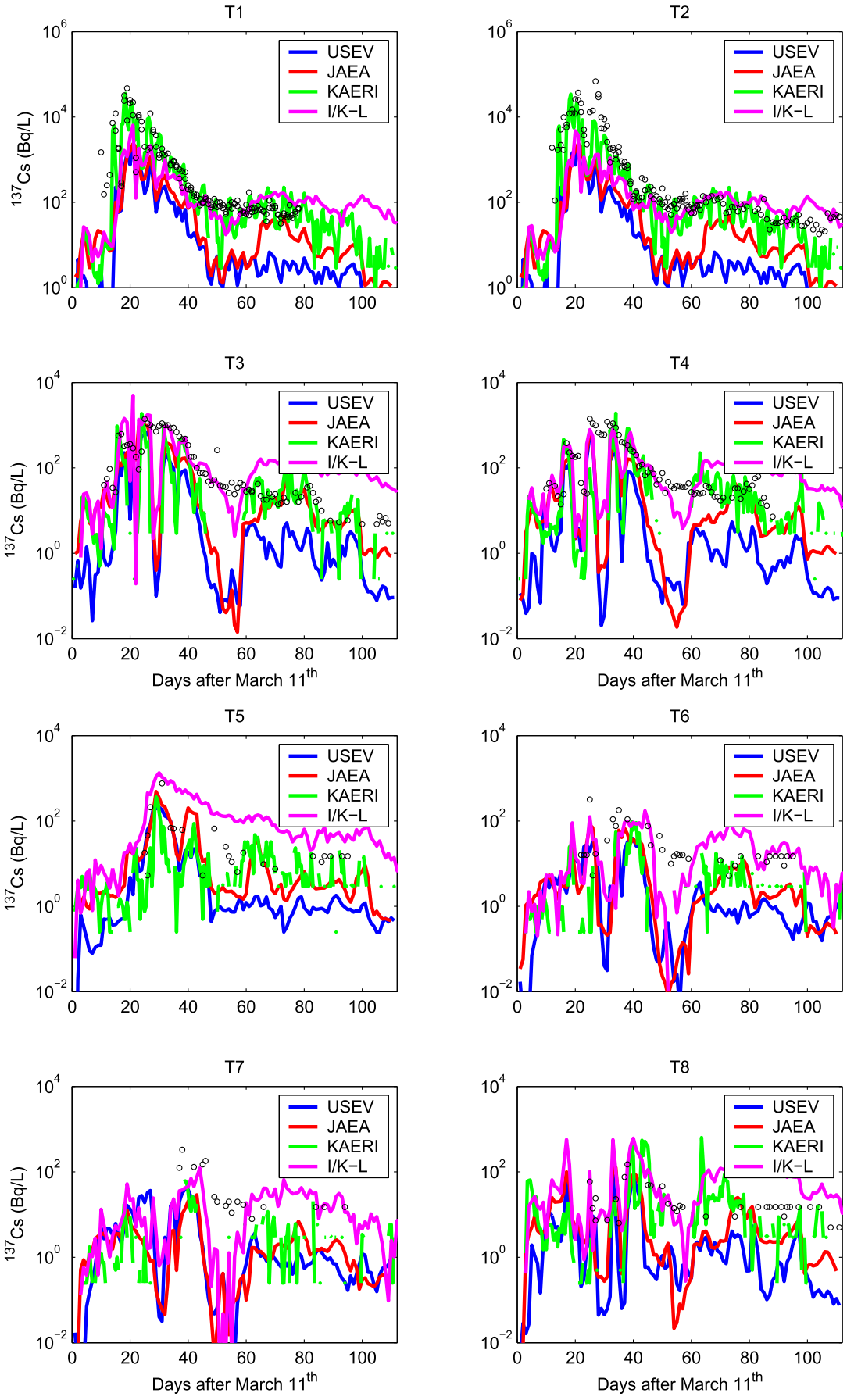

Fig. 12. Calculated and measured ^{137}Cs concentrations in surface water at points sampled by TEPCO. Exercise 4a.

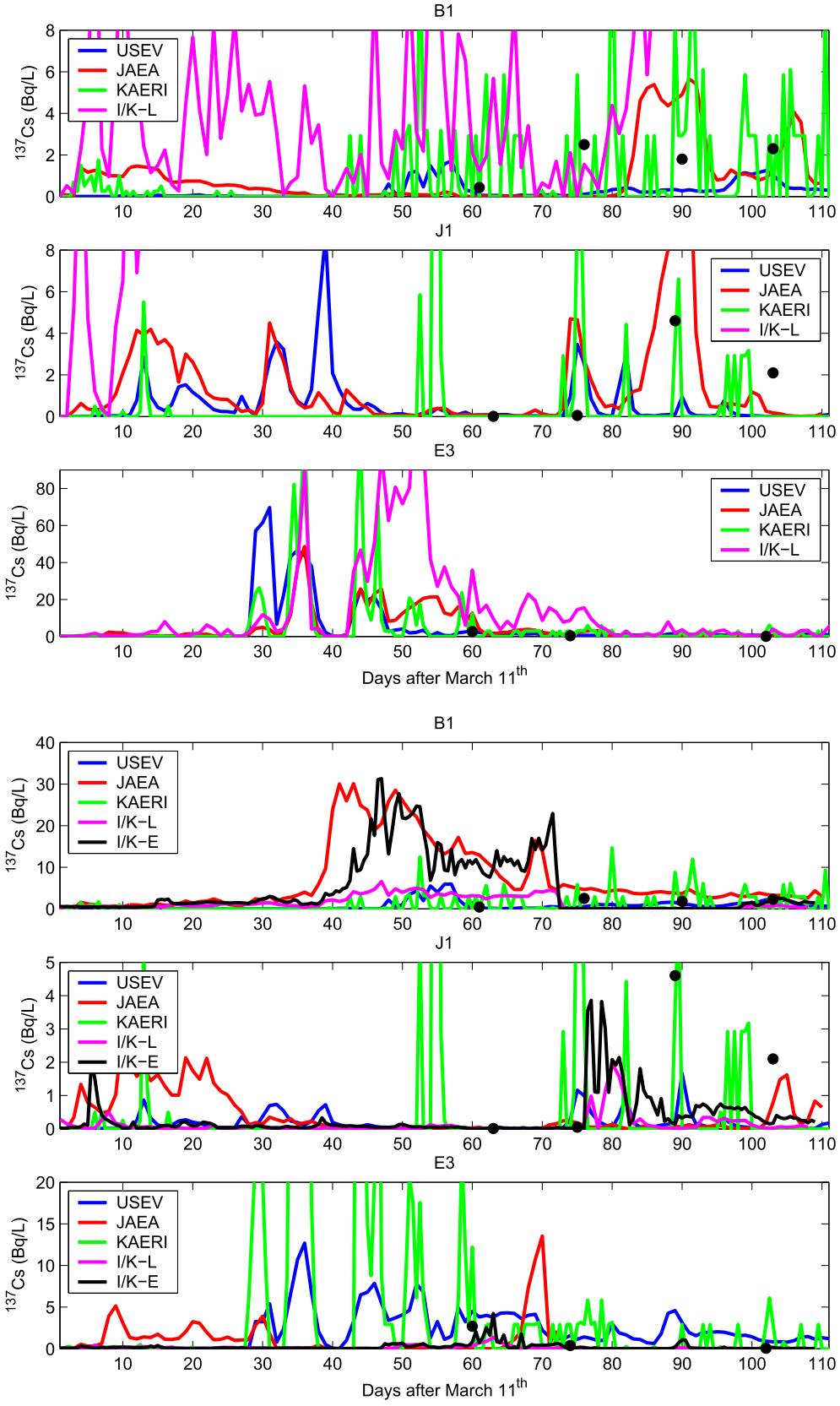

Fig. 13. Calculated and measured ^{137}Cs concentrations in surface water at points B1, J1 and E3. Top: exercise 4a; bottom: exercise 4b.

surprising that dispersion models produced so different results.

After a comparison of hydrodynamic model outputs with observed SST fields, it was concluded that a reasonable choice would be the JCOPE2 circulation. Thus, current fields produced by this hydrodynamic model were used in the following exercises.

A second dispersion exercise was carried out using a tracer and

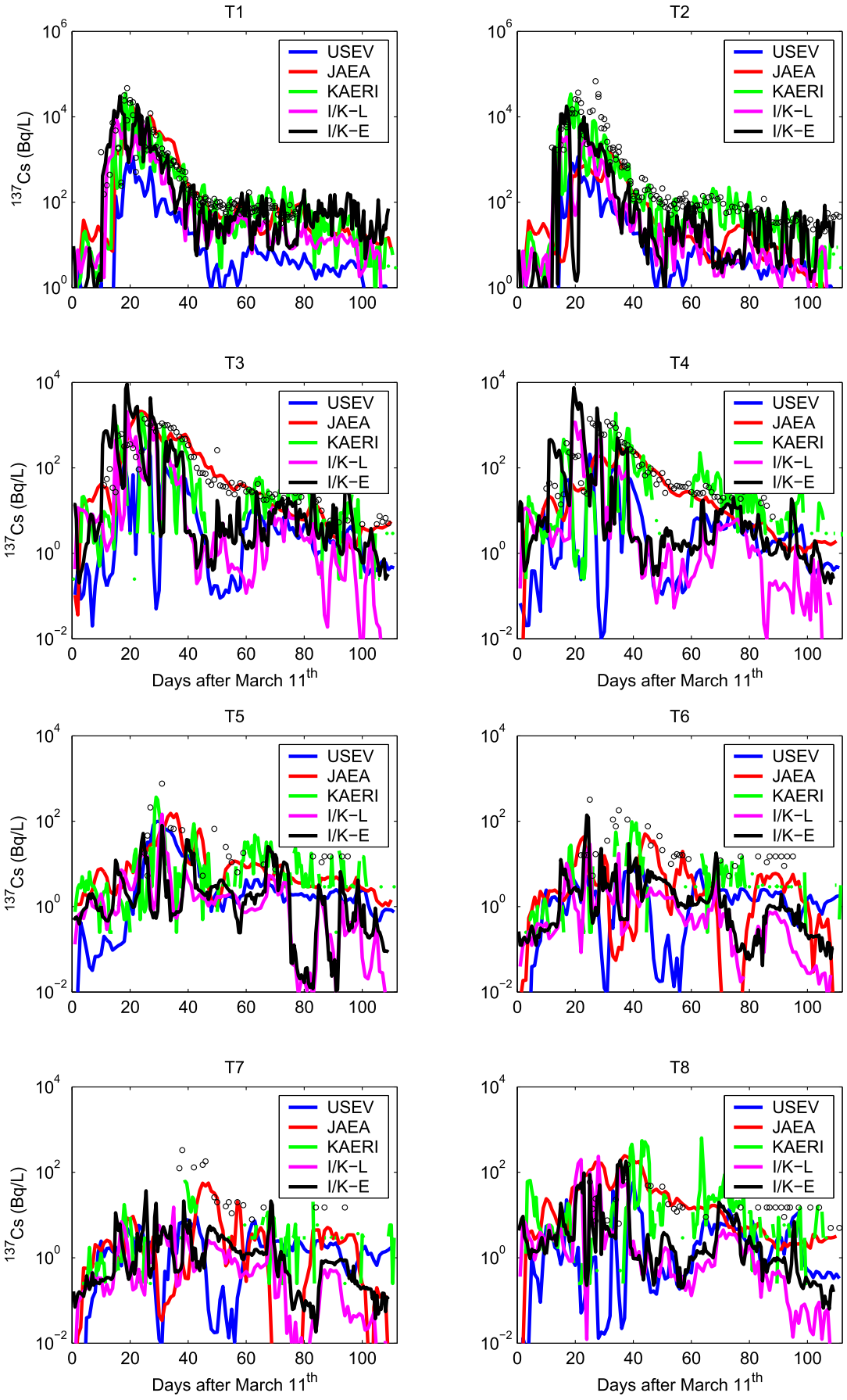

Fig. 14. Calculated and measured ^{137}Cs concentrations in surface water at points sampled by TEPCO. Exercise 4b.

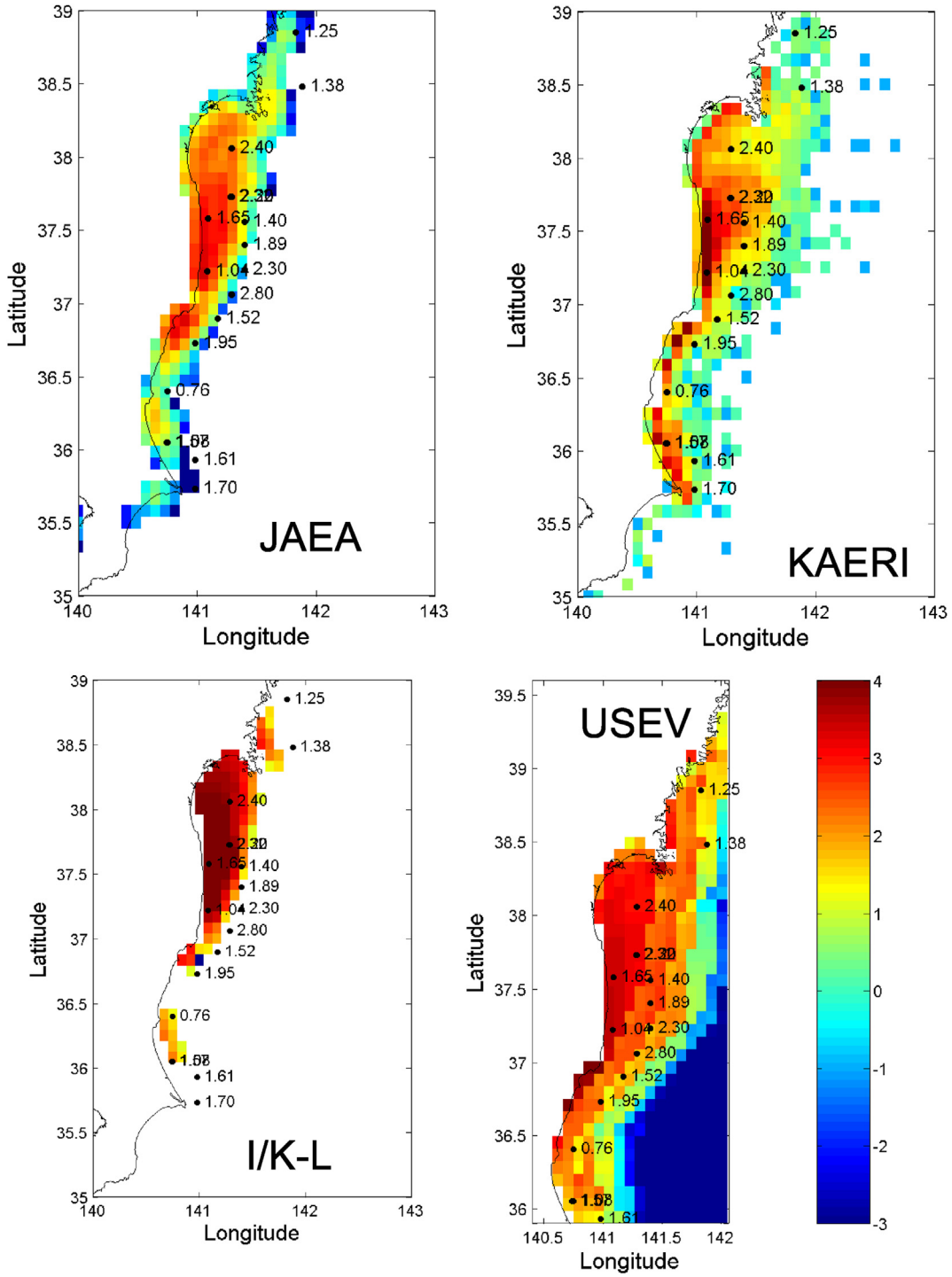

Fig. 15. ^{137}Cs in bed sediments (Bq/kg) at the end of the simulation period for exercise 4a. Logarithms of calculated and measured concentrations are drawn. The colour scale is the same for all maps.

^{137}Cs (including water/sediment interactions) and JCOPE2 circulation, as mentioned above. In the case of the tracer, model variability was significantly reduced. Results were, in general, within one order of magnitude.

In the case of ^{137}Cs, results for surface water were similar to those of the tracer, since these waters are scarcely sensitive to the presence of the seabed. Most of the variability between models was now obtained for the bed sediment. Here, in some points, results expanded again over several orders of magnitude. Nevertheless, maps of ^{137}Cs concentrations in water and sediment showed the same general features. As a consequence, it may be concluded that a significant part of the variability between models is caused by the description of hydrodynamics. Of course, in the case of ^{137}Cs in the sediment, model variability must be due to the different descriptions of water/sediment interactions used by each dispersion model.

The third exercise consisted of using the same description for water/sediment interactions in the case of ^{137}Cs. Thus, the same k_d,

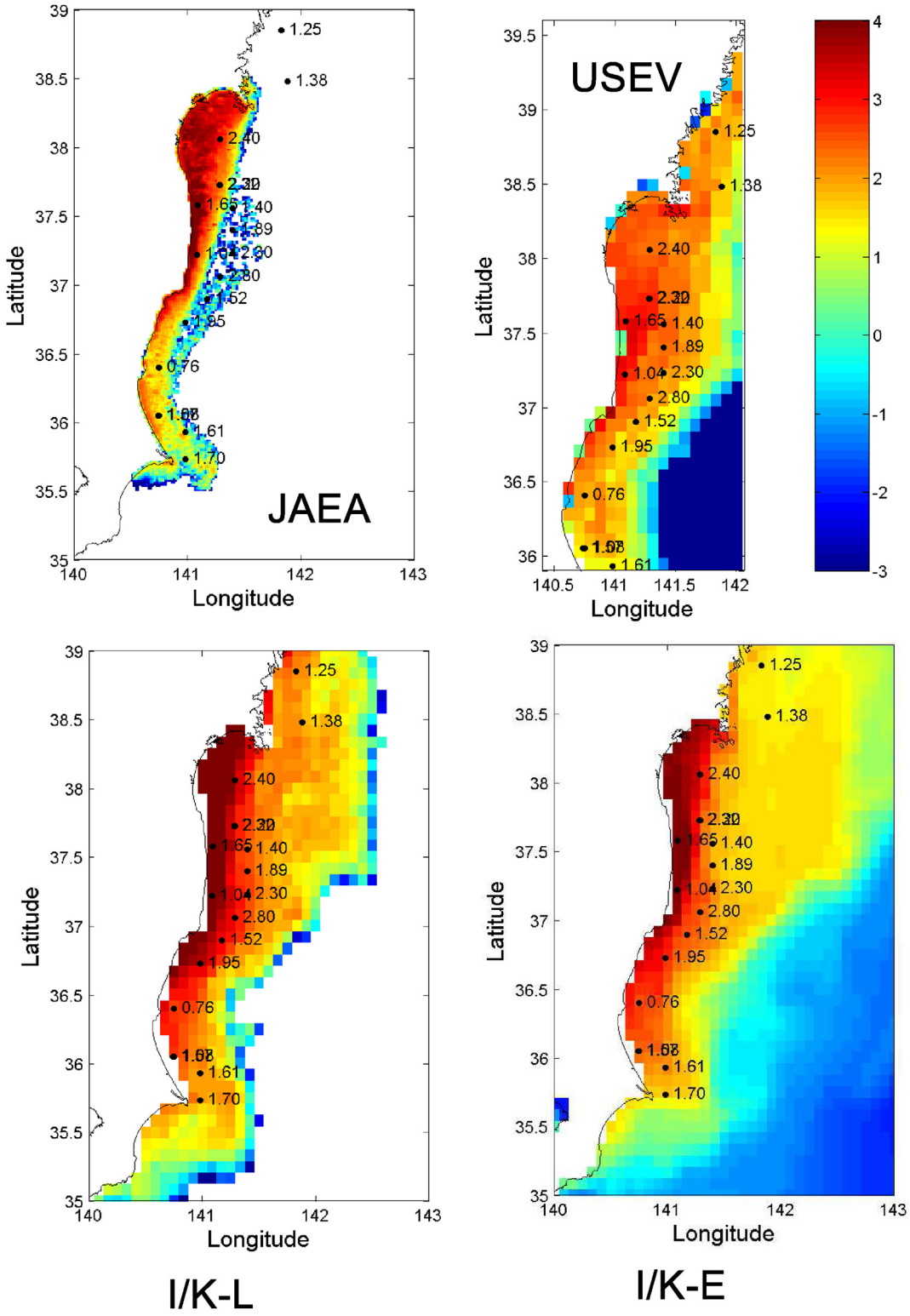

Fig. 16. ^{137}Cs in bed sediments (Bq/kg) at the end of the simulation period for exercise 4b. Logarithms of calculated and measured concentrations are drawn. The colour scale is the same for all maps.

or equivalent kinetic ratios (to be used in cases of equilibrium or dynamic models respectively), were used. An additional harmonization of models in this exercise has consisted of using the exactly the same topographic data for the Pacific Ocean and the same values for the horizontal and vertical diffusion coefficients. This exercise was again carried out for a tracer and for ^{137}Cs. In the last case, the effects of considering the presence of suspended matter in the water column was also investigated.

In the case of the tracer, agreement between models improved with respect to exercise 2. However, it seems clear that the main

factor in producing model discrepancies is water circulation, since model agreement improvement was higher from exercise 1 to 2 than from exercise 2 to 3.

In the case of ^{137}Cs, the use of the same water/sediment parameterization also led to a better agreement between model outputs in bed sediments. Calculated ^{137}Cs concentration maps in water and sediments were also similar, models producing the same behaviour. In this respect, it is also clear and obvious that a good description of contamination in the deepest water is essential for a good description of radionuclide adsorption by seabed sediments.

The presence of suspended matter in the water column did not affect the calculated dissolved concentrations. This is not surprising given the relatively low affinity of ^{137}Cs to be fixed to the solid phase and the low suspended matter concentration in open ocean waters.

At this stage, given the model harmonization which was carried out, it does not seem possible to achieve a better agreement between models. Differences in model outputs were now due to intrinsic differences between models: a) Lagrangian vs. Eulerian models and b) different numerical schemes which may be used for each model category mentioned above. In this sense, the method used to reconstruct concentrations from the density of particles in Lagrangian models may be relevant. Nevertheless, the overall agreement between models which, generally speaking, was achieved may be considered satisfactory.

All the exercises carried out considered a constant hypothetical source of radionuclides from Fukushima. The final stage of this set of simulations consisted of the use of a realistic source term. This allowed the comparisons of model outputs with ^{137}Cs measurements in water and sediments.

Generally speaking, model results were in good agreement with observations; although dissolved ^{137}Cs concentrations in surface water tended to be underestimated. It was also found that some models performed better for some target variables than for others. There was consensus between all models in the sense that contamination of the bed sediments extended over a banded area along the coast. When models were applied in exercise 4b, i.e., each team used its own water circulation and model parameterization, there was in general a very good agreement in model−model and model-data comparisons. This agreement, better than in the model−model comparisons of the very simple exercise 1, has to be attributed to some contamination due to the previous knowledge of measured data. Thus, exercise 4 was not a pure blind model test as exercises 1, 2 and 3.

It may be concluded that dispersion models are robust tools, although very sensitive to water circulation description in highly dynamic environments, as Fukushima coastal waters. If models for supporting decision-making after emergencies are designed, special care should be paid to the forcing of the dispersion model by water circulation in this type of environment. Further research in this topic is clearly required.

Acknowledgement

Work carried out in the frame of IAEA MODARIA (Modelling and Data for Radiological Impact Assessments) program. The authors are indebted to all members of MODARIA working group 10 for useful discussions held during group meetings. Work partially supported by a) EU FP7 EURATOM project PREPARE: “Innovative integrative tools and platforms to be prepared for radiological emergencies and post-accident response in Europe”, Project No. 323287. b) National Research Foundation of Korea (NRF) grant funded by the Korea government (MSIP) (MSIP: No. 2012M2A8A4025912, NSSC: No. 2012M5A1A1029210). c) V. Maderich, I. Brovchenko and K.T. Jung have been supported by CKJORC and KIOST (PE99304).

A. Hydrodynamic models

Hydrodynamic models are very briefly described in this appendix. MARS (Appendix A.5) and SYMPHONIE (appendix A.6) models also calculate dispersion.

A.1. JCOPE2, Japan Coastal Ocean Predictability Experiment

JCOPE2 (Japan Coastal Ocean Predictability Experiment) has been developed by JAMSTEC (Japan Agency of Marine-Earth Science and Technology).[3] It is based on one of the world community models, Princeton Ocean Model. Open boundary conditions are obtained from a global scale circulation model with lower resolution, using a one-way nesting procedure.

JCOPE2 consists of 23 vertical levels and spatial resolution is about 9 km. The model is driven by wind stresses, and heat and salt fluxes. The wind stress and heat flux field are calculated from the 6-hourly NCEP Global Forecast system data using bulk formulae. The salinity at the surface is restored to the monthly mean climatology with a time scale of 30 days.

The output of JCOPE2 is used for ship routing of oil tankers, fishery and drilling ships. Some examples of applications may be seen in Miyazawa et al. (2009, 2012, 2013). It has also been already applied to simulate the dispersion of Fukushima releases in the Pacific (Min et al., 2013; Periáñez et al., 2012, 2013a, 2013b).

A.2. NCOM, Navy Coastal Ocean Model

NCOM is a numerical model to produce surface currents and temperature, mixed layer depth, current and thermohaline profiles in global scale (Barron et al., 2006). NCOM is a free surface, primitive-equation model and having a curvilinear horizontal grid. Horizontal resolution varies from 19.5 km near the equator to 8 km in the Arctic, with mid-latitude resolution of about 1/8° latitude (~14 km). The hybrid sigma/z vertical schemes are adopted with 19 terrain following sigma-levels in the upper 137 m, and 21 fixed-thickness $z-$ levels extending to a maximum depth of 5500 m. NCOM extends from the Arctic Ocean to the coast of Antarctica and from the open ocean over the shelf break to near-shore regions. The present daily model run consists of a 72-h hindcast to assimilate fields that include recent observations, and a 72-h forecast. Global NCOM produced sea surface height, salinity, temperature, u-velocity and v-velocity. Global NCOM can include atmospheric forcing, but it does not include tidal heights and currents.

Global NCOM was retired on 5 April 2013 and replaced by operational 1/12° HYCOM. Especially, after the Fukushima accident, three hour averaged three-dimensional currents near Fukushima region were produced from NCOM, operated by the US Navy operational global Nowcast/Forecast system from March 12 to June 30, 2011. There were 40 vertical levels and the spatial resolution was 1 km.

A.3. HYCOM, Hybrid Coordinate Ocean Model

HYCOM consortium is a multi-institutional effort sponsored by the National Ocean Partnership (NOPP) as a part of U.S. Global Ocean Data Assimilation Experiment (GODAE) (Bleck, 2001). HYCOM is a primitive equation, general circulation model with vertical coordinates that remain isopycnic in the open, stratified ocean.

Computations in global HYCOM are carried out on a Mercator

[3] http://www.jamstec.go.jp/frcgc/jcope/htdocs/e/jcope_system_description.html.

grid between 78° S and 47° N (1/12° horizontal resolution at the equator). A bipolar patch is used for regions north of 47° N. The horizontal dimensions of the global grid are 4500 × 3298 grid points resulting in ~7 km spacing on average. There are 33 vertical layers. Surface forcing includes wind stress, wind speed, heat flux and precipitation. HYCOM uses the Navy Coupled Ocean Data Assimilation System (NCODA) in U.S. for data assimilation. The outputs are surface heat flux, sea surface height, surface salinity trend, surface temperature trend, salinity, potential temperature, u-velocity and v-velocity. Global HYCOM can include atmospheric forcing, but it does not include tidal heights and currents.

A.4. Kyoto University

The coastal model was developed by Kyoto University, the Japan Agency for Marine-Earth Science and Technology (JAMSTEC), and the Japan Marine Science Foundation (Kawamura et al., 2011). A nesting method enables downscale calculation from the largest area, that covers the northwestern part of North Pacific with horizontal resolutions of 1/8° in latitude and 1/6° in longitude, to the 2-step-nested finer domain around the Fukushima area, with horizontal resolutions of 1/72° in latitude and 1/54° in longitude (approximately 1.5 km). The model domain for the coastal model extends from 140.5° E to 144° E longitude and from 35.5° N to 38.5° N latitude. There are 78 layers set in the vertical. The four-dimensional variation (4D-VAR) method was applied for outermost model to obtain the reanalysis data.

A.5. MARS3D, IFREMER (France)

Circulation modelling was performed using the operational MARS-3D code (3D hydrodynamical Model for Applications at Regional Scale) developed by IFREMER (French Research Institute for Exploitation of the Sea). This is a three-dimensional model with reduced sigma vertical coordinates based on the resolution of the Navier–Stokes equations (Lazure and Dumas, 2008). This model with free surface resolves primitive equations using a time-splitting scheme under assumptions of Boussinesq approximation, hydrostatic equilibrium and incompressibility.

Application to Fukushima area is described in Bailly du Bois et al. (2014). The model domain covers the oceanic area off Fukushima: 31°N – 43.2°N, 137°E – 150°E (1000 km × 1200 km). The horizontal resolution is 1/60°(one nautical mile), in both E–W and N–S directions, with 742 grid cells in the E–W direction and 622 in the N–S direction. The vertical resolution of the sigma coordinate is 40 layers refined near the surface. Bathymetric data are derived from JODC.

Wind forcing, water and heat flux are downscaled from the atmospheric forecast and hindcast of the National Centers for Environmental Prediction (NCEP) meteorological global model (http://www.ncep.noaa.gov/) with a resolution of 1/2°. At the scale of thermohaline and geostrophic effects, the initial and boundary conditions are derived from the daily oceanic forecast and hindcast of the global model proposed by Mercator-Ocean with a resolution of 1/12° (http://www.mercator-ocean.fr/). For the downscaling procedure, the temperature, salinity, currents and sea level are interpolated in both time and space to provide initial and boundary conditions. The tide at open boundary conditions is prescribed using 16 tidal harmonic components from the FES2004 numerical atlas with a horizontal resolution of 1/8°.

Radionuclide dispersion is calculated using an Eulerian method. The parallelized MARS3D code runs on 256 MPI ranks for the present Fukushima application.

A.6. SYMPHONIE (SIROCCO, University of Toulouse, France)

The used model is the non-hydrostatic ocean model following the Boussinesq hydrostatic SYMPHONIE model developed by the Sirocco system team. Both are using an Arakawa type finite difference method for the C grid. The principal equations of the physical engine are detailed in Marsaleix et al. (2006, 2009). The physical and numerical options (Non-Hydrostatic, free surface, generalized coordinates combined to an ALE method) are particularly suitable for the coastal area.

Modelling has been performed at the request of the International Atomic Energy Agency. The complete description and results are available in Estournel et al. (2012).

The model uses a stretched horizontal grid with a variable horizontal resolution, from 600 m × 600 m at the nearest grid point from Fukushima, to 5 km × 5 km offshore. The vertical grid is based on a generalized s-coordinate system. The 30 vertical levels are irregularly distributed, with increased resolution near the sea surface.

The model was initialized and forced at its lateral boundaries with the global NCOM real-time operational ocean model of the U.S. Navy (Barron et al., 2006) operated by NOAA. At the sea surface, the ocean model is forced by the meteorological fluxes delivered every 3 h by ECMWF. The tidal forcing at the lateral open boundaries is provided by the T-UGO model, implemented for this purpose by the SIROCCO team on the Japanese Pacific coast. The main rivers of the region (between 35.5° and 38.5° N), the Tone to the south, and the Natori and Abukuma to the north, were introduced into the model on the basis of climatological freshwater discharges (190, 17 and 67 m^3/s respectively).

The model was initialized on 2011 February 21st. Currents and vertical diffusivities computed by the model were averaged over 3 h periods and stored to compute the advection and diffusion of tracers in off-line mode, using an Eulerian representation. An inverse-method calculation was carried out to estimate the source term.

A.7. SELFE

The 3D circulation hydrostatic model SELFE (Zhang and Battista, 2008; Roland et al., 2012) renamed now as SCHISM (http://ccrm.vims.edu/schism/) is an open-source community-supported modelling system based on unstructured grids, designed for seamless simulation of 3D baroclinic circulation across the scales. It solves Reynolds-stress averaged Navier–Stokes (RANS) equations using the Generic Length Scale (GLS) turbulence closure by Umlauf and Burchard (2003). The circulation model is coupled with the spectral wave WWMII and a sediment transport model. In the multi-fraction sediment transport model the non-cohesive sediment flux due to sediment deposition is simulated as a flux of particles that fall down with a settling velocity. The erosion flux is calculated using van Rijn (1984a, 1984b) formulations. For the cohesive sediments, a deposition flux appears only if the shear stress is lower than the critical shear stress for deposition. The erosion flux for cohesive sediments is formulated following Ariathurai and Arulanandan (1978). For the mixture of cohesive and non-cohesive sediments the model follows the assumptions made by van Ledden (2003). The Winterwerp and van Kesteren (2004) equilibrium model is used to calculate floc size and settling velocity.

The calculation mesh for the northwestern Pacific Ocean simulations contains 49,700 nodes and 97,989 triangular elements and has resolution from approximately 500 m near the Fukushima Daiichi NPP to 10 km in the NW Pacific. The surface forcing is obtained from ERA Interim reanalysis. The lateral boundary conditions for SELFE calculations were obtained from HYCOM nowcast/forecast

system. The SELFE temperature was nudged towards the HYCOM fields. The tidal forcing is imposed at open boundaries using NAO.99b tidal prediction system.

B. IMMSP/KIOST model

The model developed by IMMSP/KIOST for radionuclide transport may run in two modes: Eulerian (I/K-E) and Lagrangian (I/K-L). Water circulation and sediment transport is obtained from SELFE model (appendix A.7).

The Eulerian radionuclide transport model in describes the key exchange processes in the system of water-multi-class sediments. In the water column radionuclides in dissolved and particulate phases are transported by currents (advection processes) with the simultaneous influence of the turbulent diffusion processes. The radionuclides in dissolved phase interact with the particulate phase (suspended sediments and bottom deposits). The transfer of activity between the dissolved and particulate phases is described by adsorption−desorption processes in terms of the desorption rates and the distribution coefficients for the water column and for the bottom deposit. The distribution coefficient is written as a function of the particle size following Periáñez (2005). The settling of contaminated suspended sediments and the bottom erosion are important pathways of radionuclide exchanges between bottom and suspended sediments. The transfer of activity between the water column and the pore water in the upper layer of the bottom sediment is governed by a diffusion processes.

In the Lagrangian model a release of radioactivity is simulated by a large number of particles, each of them transport an equal amount of activity. We use the same equations as for Eulerian model but for only one characteristic fraction of sediments. The particles are transported by currents, turbulent diffusion and they can settle with sediment particles. The turbulent diffusion, transfer of activity between solute, particulate and bottom phases and decay are described by stochastic methods (Periáñez and Elliott, 2002).

C. LORAS model (KAERI)

An oceanic dispersion model named LORAS (Lagrangian Oceanic Radiological Assessment System) has been developed by Korea Atomic Energy Research Institute to evaluate the transport characteristics of the radionuclides released into the sea for a nuclear accident (Min et al., 2013).

The model was designed to calculate radionuclide concentrations in seawater, suspended matter and seabed sediments in time and space using a particle tracking method. The particle tracking technique has some advantages over finite difference methods. In particular, numerical diffusion is not introduced and the exact position of the release point may be specified. Thus, it is not necessary to assume that the discharge is instantaneously mixed into a grid cell of a given size. A passive particle is transported by current components and dispersed by turbulent motion. Currents are supplied by the hydrodynamic circulation model and turbulent dispersion is evaluated using a random walk method (Min et al., 2013, 2014). The dispersion of reactive and non-reactive radionuclides may also be simulated in the model. Three dimensional turbulent diffusion and the pollutant interactions between water, suspended matter and bottom sediments are simulated using a stochastic method (Periáñez and Elliott, 2002). These processes are formulated using kinetic transfer coefficients, considering that exchanges of radionuclides between the liquid and solid phases are governed by a first-order reversible reaction.

D. Sisbahia (Instituto de Engenheria Nuclear)

A comprehensive description of SisBAHIA can be found on the pertinent references (Rosman, 2001; Cunha and Rosman, 2005; Lamego, 2013a, 2013b; Saad, 1994). In short, the current version has the following main features:

Hydrodynamic model: it is a constant density 3D/2DH hydrodynamic circulation model optimized for natural water bodies. Results can be either three-dimensional (3D) or vertically averaged (2DH) depending on input data. "Optimized" is used in the sense of a model planned for optimal representation of flows in natural water bodies. Calibration process is minimized due to: spatial discretization via quadratic finite elements and σ transformation, allowing optimal representation of water bodies with complex geometries and bottom topography; wind field and bottom roughness that can vary dynamically in time and space, and self-adjusting multi-scale turbulence modelling based on Large Eddy Simulation. A wind-wave generation model is included.

Eulerian transport model: it is a general purpose advective-diffusive transport model with kinetic reactions, for 2DH or selected layers of 3D flows with a given thickness. This model can be used to compute space distribution and fate of dissolved contaminants. A set of Eulerian transport models for the coupled simulation of water quality parameters is also included.

Lagrangian transport model − deterministic mode: it is a general purpose advective diffusive transport model with kinetic reactions for selected layers of 3D and for 2DH flows. This model is especially suitable for the simulation of plumes or clouds that are initially small to be well resolved by the discretizing mesh of the associated hydrodynamic model. Any curve representing a kinetic reaction dependent on the lifetime of a given particle can be adopted. The user can choose to run the model in free transport mode or conditioned transport mode. The latter is particularly suitable for simulations of sedimentological processes. The transport can be conditioned by a minimum velocity, minimum bottom stress due to currents or due to currents and wind waves. The user can specify a tolerance band for the limiting condition, in which the transport of a particle follows a fuzzy decision process. In addition, this model may also run in probabilistic mode.

E. SEA-GEARN (JAEA)

A particle random-walk model, SEA-GEARN (Kobayashi et al., 2007), has been used to simulate radionuclide transport model in the Pacific Ocean. SEA-GEARN uses three-dimensional velocity data calculated by an ocean general circulation model as the input variables. If non-conservative radionuclides are concerned, the interactions with particulate matter must be considered. To take these situations into account, a new model that solves three-phase interaction, developed by Periáñez (Periáñez and Elliott, 2002), was adopted in SEA-GEARN. Radionuclides are assumed to exist in three phases, such as dissolved, large particulate matter (LPM) and active bottom sediment. The LPM is an aggregate which has a single radius and density.

The following assumptions are made: (1) the dissolved phase consists of radionuclides that are dissolved and adsorbed onto fine (diameter <0.8 μm) particles without settling velocity, (2) the LPM phase consists of radionuclides that are adsorbed on settling suspended particles, (3) the active bottom sediment phase consists of radionuclides that are adsorbed on the LPM phase and deposit on the seabed. These particles may re-suspend according to the

bottom water velocity. Kinetic transfer coefficients are used for the calculation of adsorption/desorption between dissolved phase and LPM phase or between dissolved phase and seabed sediment phase (Periáñez, 2003b).

F. USEV-3D model

This model is based on the three-dimensional advection/diffusion dispersion equations. Water circulation has been obtained from JCOPE2 hydrodynamic model (Periáñez et al., 2012, 2013a, 2013b). Daily three-dimensional currents are imported to solve the advective transport of radionuclides.

There has been evidence to suggest that uptake takes place in two stages: fast surface adsorption followed by slow migration of ions to pores and interlattice spacings (Nyffeler et al., 1984; Ciffroy et al., 2001; El Mrabet et al., 2001). Consequently, two kinetic models have been tested in the Fukushima application. The 1-step model considers that exchanges of radionuclides between water and sediments are governed by a first-order reversible reaction, being k_1 and k_2 the forward and backward rates respectively. The 2-step model considers that exchanges are governed by two consecutive reversible reactions: surface adsorption is followed by another process that may be a slow diffusion of ions into pores and interlattice spacings, inner complex formation or a transformation such as an oxidation. k_3 and k_4 are forward and backward rates for this second reaction. Thus, sediments are divided in two phases: a reversible and a slowly reversible fraction. It has been shown that the 2-step model reproduces both the adsorption and release kinetics of ^{137}Cs in the Irish Sea, where it is released from Sellafield nuclear fuel reprocessing plant (Periáñez, 2003a).

In a previous work (Periáñez et al., 2012) concerning the dispersion of ^{137}Cs released from Fukushima it was found that the 2-step model reproduced measured ^{137}Cs concentrations in bed sediments better than the 1-step model. Consequently, the 2-step model has been used in all Fukushima exercises involving this radionuclide, except when common parameters for all models are defined (exercise 3 and 4a).

Some parameters are required to simulate ^{137}Cs dispersion. Rates k_2, k_3 and k_4 are taken from previous works dealing with dispersion of this radionuclide (Periáñez, 2004, 2008). Although it is true that kinetic rates are site-specific, there is not information about them in Japan Pacific Ocean coastal waters. Thus, representative values already used in the English Channel and Western Mediterranean Sea have been used as a first order approximation. As discussed before (Periáñez, 2003a, 2004, 2008, 2009), the kinetic rate k_1 can be deduced from rates mentioned above and the radionuclide distribution coefficient k_d. The mean value of the measured Cs distribution coefficient in Japanese coastal water is 2.1×10^3 (Honda et al., 2012), comparable to the IAEA (2004) recommended value. We have fixed $k_d = 2 \times 10^3$ to deduce k_1 following the procedure described in such references. The distribution of fine sediments in the seabed has been reconstructed from information in Saito (1989).

References

Ariathurai, R., Arulanandan, K., 1978. Erosion rates of cohesive soils. ASCE J. Hydraul. Div. 104 (2), 279–283.

Bailly du Bois, P., Laguionie, P., Boust, D., Korsakissok, I., Didier, D., Fiéve, B., 2012. Estimation of marine source-term following Fukushima Dai-ichi accident. J. Environ. Radioact. 114, 2–9.

Bailly du Bois, P., Garreau, P., Laguionie, P., Korsakissok, I., 2014. Comparison between modelling and measurement of marine dispersion, environmental half-time and 137-Cs inventories after the Fukushima Daiichi accident. Ocean. Dyn. 64, 361–383.

Barron, C.N., Kara, A.B., Martin, P.J., Rhodes, R.C., Smedstad, L.F., 2006. Formulation, implementation and examination of vertical coordinate choices in the global Navy Coastal Ocean Model (NCOM). Ocean. Model. 11 (3–4), 347–375.

Behrens, E., Schwarzkopf, F.U., Lubbecke, J., Boning, C.W., 2012. Model simulations on the long-term dispersal of ^{137}Cs released into the Pacific Ocean off Fukushima. Environ. Res. Lett. 7, 034000 (10 pp.).

Black, E.E., Buesseler, K.O., 2014. Spatial variability and the fate of cesium in coastal sediments near Fukushima, Japan. Biogeosciences 11, 5123–5137.

Bleck, R., 2001. An oceanic general circulation model framed in hybrid isopycnic-Cartesian coordinates. Ocean. Model. 4, 55–88.

Choi, Y., Kida, S., Takahashi, K., 2013. The impact of oceanic circulation and phase transfer on the dispersion of radionuclides released from the Fukushima Dai-ichi Nuclear Power Plant. Biogeosciences 10, 4911–4925.

Ciffroy, P., Garnier, J.M., Pham, M.K., 2001. Kinetics of the adsorption and desorption of radionuclides of Co, Mn, Cs, Fe, Ag and Cd in freshwater systems: experimental and modelling approaches. J. Environ. Radioact. 55, 71–91.

Cunha, C.L.N., Rosman, P.C.C., 2005. A semi-implicit finite element model for natural water bodies. Water Res. 39, 2034–2047.

Dietze, H., Kriest, I., 2012. ^{137}Cs off Fukushima Dai-ichi, Japan. Model based estimates of dilution and fate. Ocean Sci. 8, 319–332.

Duursma, E.K., Carroll, J., 1996. Environmental Compartments. Springer, Berlin.

El Mrabet, R., Abril, J.M., Manjón, G., García-Tenorio, R., 2001. Experimental and modelling study of plutonium uptake by suspended matter in aquatic environments from southern Spain. Water Res. 35, 4184–4190.

Estournel, C., Bosc, E., Bocquet, M., Ulses, C., Marselaix, P., Winiarek, V., Osvath, I., Nguyen, C., Duhaut, T., Lyard, F., Michaud, H., Auclair, F., 2012. Assessment of the amount of 137-Cs released into the Pacific Ocean after the Fuskushima accident and analysis of its dispersion in Japanase coastal waters. J. Geophys. Res. 117, C1014.

Gifford, F.A., 1982. Horizontal diffusion in the atmosphere: a Lagrangian-dynamical theory. Atmos. Environ. 16, 505–512.

Honda, M., Aono, T., Aoyama, M., Hamajima, Y., Kawakami, H., Kitamura, M., Masumoto, Y., Miyazawa, Y., Takigawa, M., Saino, T., 2012. Dispersion of artificial caesium-134 and -137 in the western North Pacific one month after the Fukushima accident. Geochem. J. 46, 1–9.

IAEA, 1996. An Overview of the BIOMOVS-ii Study and its Findings. Technical Report 17. Vienna.

IAEA, 2000. Modelling of the Transfer of Radiocaesium from Deposition to Lake Ecosystems. Report of the VAMP Aquatic Working Group. IAEA-tecdoc-1143 (Vienna).

IAEA, 2012. Environmental Modelling for Radiation Safety (EMRAS) – a Summary Report of the Results of the EMRAS Programme (2003-2007). IAEA-TECDOC-1678. Vienna.

IAEA, 2004. Sediment Distribution Coefficients and Concentration Factors for Biota in the Marine Environment. Technical Reports Series 422. Vienna.

Jayne, S.R., Hogg, N.G., Waterman, S.N., Rainville, L., Donohue, K.A., Randolph Watts, D., Tracey, K.L., McClean, J.L., Maltrud, M.E., Qiu, B., Chen, S., 2009. The Kuroshio extension and its recirculation gyres. Deep Sea Res. Part I 56 (12), 2088–2099.

Kawamura, H., Kobayashi, T., Furuno, A., In, T., Ishikawa, Y., Nakayama, T., Shima, S., Awaji, T., 2011. Preliminary numerical experiments on oceanic dispersion of ^{131}I and ^{137}Cs discharged into the ocean because of the Fukushima Daiichi nuclear power plant disaster. J. Nucl. Sci. Technol. 48, 1349–1356.

Kawamura, H., Kobayashi, T., Furuno, A., Usui, N., Kamachi, M., 2014. Numerical simulation on the long-term variation of radioactive cesium concentration in the North Pacific due to the Fukushima disaster. J. Environ. Radioact. 136, 64–75.

Kobayashi, T., Otosaka, S., Togawa, O., Hayashi, K., 2007. Development of a nonconservative radionuclides dispersion model in the ocean and its application to surface cesium-137 dispersion in the Irish Sea. J. Nucl. Sci. Technol. 44 (2), 238–247.

Kobayashi, T., Nagai, H., Chino, M., Kawamura, H., 2013. Source term estimation of atmospheric release due to the Fukushima Dai-ichi Nuclear Power Plant accident by atmospheric and oceanic dispersion simulations. J. Nucl. Sci. Technol. 50, 255–264.

Lamego, F.F., 2013a. Advanced nuclear reactors and Tritium impacts: modeling the aquatic pathway. Prog. Nucl. Energy 68, 9–22.

Lamego, F.F., 2013b. Eulerian modeling of radionuclides in surficial water: the case of Ilha Grande Bay (RJ, Brazil). In: Integral Methods in Science and Engineering, first ed. Springer, New York, pp. 259–277.

Lazure, P., Dumas, F., 2008. An external-internal mode coupling for a 3D hydrodynamical model for applications at regional scale (MARS). Adv. Water Resour. 31 (2), 233–250.

Li, Y.H., Burkhardt, L., Buchholtz, M., O'Hara, P., Santschi, P.H., 1984. Partition of radiotracers between suspended particles and seawater. Geochim. Cosmochim. Acta 48, 2011–2019.

Maderich, V., Bezhenar, R., Heling, R., Jung, K.T., Myoung, J.G., Cho, Y.-K., Qiao, F., Robertson, L., 2014a. Regional long-term model of radioactivity dispersion and fate in the Northwestern Pacific and adjacent seas: application to the Fukushima Dai-ichi accident. J. Environ. Radioact. 131, 4–18.

Maderich, V., Jung, K.T., Bezhenar, R., de With, G., Qiao, F., Casacuberta, N., Masqué, P., Kim, Y.H., 2014b. Dispersion and fate of ^{90}Sr in the Northwestern Pacific and adjacent seas: global fallout and the Fukushima Dai-ichi accident. Sci. Total Environ. 494–495, 261–271.

Marsaleix, P., Auclair, F., Estournel, C., 2006. Considerations on open boundary conditions for regional and coastal ocean models. J. Atmos. Ocean. Technol. 23, 1604–1613.

Marsaleix, P., Auclair, F., Estournel, C., 2009. Low-order pressure gradient schemes in sigma coordinate models: the seamount test revisited. Ocean. Model. 30, 169–177.

Martazinova, V., 2005. The classification of synoptic patterns by method of analogs. J. Environ. Eng. 7, 61–65.

Masumoto, Y., Miyazawa, Y., Tsumune, D., Tsubono, T., Kobayashi, T., Kawamura, H., Estournel, C., Marseleix, P., Lanerolle, L., Mehra, A., Garraffo, Z.D., 2012. Oceanic dispersion simulations of ^{137}Cs released from the Fukushima Daiichi nuclear power plant. Elements 8, 207–212.

Mellor, G.L., Yamada, T., 1982. Development of a turbulence closure model for geophysical fluid problems. Rev. Geophys. 20, 851–875.

Min, B.I., Periáñez, R., In-Gyu, Kim, Kyung-Suk, Suh, 2013. Marine dispersion assessment of ^{137}Cs released from the fukushima nuclear accident. Mar. Pollut. Bull. 72, 22–33.

Min, B.I., Periáñez, R., Park, K., In-Gyu, Kim, Kyung-Suk, Suh, 2014. Assessment in marine environment for a hypothetic nuclear accident based on the database of tidal harmonic constants. Mar. Pollut. Bull. 87, 269–275.

Miyazawa, Y., Zhang, R., Guo, X., Tamura, H., Ambe, D., Lee, J.S., Okuno, A., Yoshinari, H., Setou, T., Komatsu, K., 2009. Water mass variability in the western North Pacific detected in a 15-year eddy resolving ocean reanalysis. J. Oceanogr. 65, 737–756.

Miyazawa, Y., Masumoto, Y., Varlamov, S.M., Miyama, T., 2012. Transport simulation of the radionuclide from the shelf to the open ocean around Fukushima. Cont. Shelf Res. 50–51, 16–29.

Miyazawa, Y., Masumoto, Y., Varlamov, S.M., Miyama, T., Takigawa, M., Honda, M., Saino, T., 2013. Inverse estimation of source parameters of oceanic radioactivity dispersion models associated with the Fukushima accident. Biogeosciences 10, 2349–2363.

Monte, L., Hakanson, L., Periáñez, R., Laptev, G., Zheleznyak, M., Maderich, V., Koshebutsky, V., 2006. Experiences from a case study of multi-model application to assess the behaviour of pollutants in the Dnieper-Bug estuary. Ecol. Model. 195, 247–263.

Monte, L., Boyer, P., Brittain, J., Goutal, N., Heling, R., Kryshev, A., Kryshev, I., Laptev, G., Luck, M., Periáñez, R., Siclet, F., Zheleznyak, M., 2008. Testing models for predicting the behaviour of radionuclides in aquatic systems. Appl. Radiat. Isot. 66, 1736–1740.

Nakano, M., Povinec, P., 2012. Long-term simulations of the ^{137}Cs dispersion from the Fukushima accident in the world ocean. J. Environ. Radioact. 111, 109–115.

Nyffeler, U.P., Li, Y.H., Santschi, P.H., 1984. A kinetic approach to describe trace element distribution between particles and solution in natural aquatic systems. Geochim. Cosmochim. Acta 48, 1513–1522.

Oikawa, S., Takata, H., Watabe, T., Misonoo, J., Kusakabe, M., 2013. Distribution of the Fukushima-derived radionuclides in seawater in the Pacific off the coast of Miyagi, Fukushima, and Ibaraki Prefectures, Japan. Biogeosciences 10, 5031–5047.

Periáñez, R., 2003a. Kinetic modelling of the dispersion of plutonium in the eastern Irish Sea: two approaches. J. Mar. Syst. 38, 259–275.

Periáñez, R., 2003b. Redissolution and long-term transport of radionuclides released from a contaminated sediment: a numerical modelling study. Estuarine. Coast. Shelf Sci. 56 (1), 5–14.

Periáñez, R., 2004. Testing the behaviour of different kinetic models for uptake-release of radionuclides between water and sediments when implemented on a marine dispersion model. J. Environ. Radioact. 71, 243–259.

Periáñez, R., 2005. Modelling the Dispersion of Radionuclides in the Marine Environment: an Introduction. Springer, Berlin.

Periáñez, R., 2008. A modelling study on ^{137}Cs and ^{239,240}Pu behaviour in the Alborán Sea, western Mediterranean. J. Environ. Radioact. 99, 694–715.

Periáñez, R., 2009. Environmental modelling in the Gulf of Cádiz: heavy metal distributions in water and sediments. Sci. Total Environ. 407, 3392–3406.

Periáñez, R., Elliott, A.J., 2002. A particle-tracking method for simulating the dispersion of non-conservative radionuclides in coastal waters. J. Environ. Radioact. 58 (1), 13–33.

Periáñez, R., Kyung-Suk, Suh, Byung-Il, Min, 2012. Local scale marine modelling of Fukushima releases. Assessment of water and sediment contamination and sensitivity to water circulation description. Mar. Pollut. Bull. 64, 2333–2339.

Periáñez, R., Suh, Kyung-Suk, Min, Byung-Il, Casacuberta, N., Masqué, P., 2013a. Numerical modelling of the releases of ^{90}Sr from Fukushima to the ocean: an evaluation of the source term. Environ. Sci. Technol. 47, 12305–12313.

Periáñez, R., Suh, Kyung-Suk, Min, Byung-Il, 2013b. Should we measure plutonium concentrations in marine sediments near Fukushima? J. Radioanal. Nucl. Chem. 298, 635–638.

Periáñez, R., Bezhenar, R., Iosjpe, M., Maderich, V., Nies, H., Osvath, I., Outola, I., de With, G., 2014. A comparison of marine radionuclide dispersion models for the Baltic Sea in the frame of IAEA MODARIA program. J. Environ. Radioact. 139, 66–77.

Roland, A., Zhang, Y.J., Wang, H.V., Meng, Y., Teng, Y.C., Maderich, V., Brovchenko, I., Dutour-Sikiric, M., Zanke, U., 2012. A fully coupled 3D wave-current interaction model on unstructured grids. J. Geophys. Res. 117, 1–18. http://dx.doi.org/10.1029/2012JC007952. C00J33.

Rosman, P.C.C., 2001. Modeling shallow water bodies via filtering techniques. Numer. Methods Water Resour. 5, 1–162.

Rossi, V., Sebille, E., Gupta, A.E., Garçon, V., England, M.H., 2013. Multi-decadal projections of surface and interior pathways of the Fukushima Cesium-137 radioactive plume. Deep Sea Res. I 80, 37–46.

Rossi, V., Sebille, E., Gupta, A.E., Garçon, V., England, M.H., 2014. Corrigendum to multi-decadal projections of surface and interior pathways of the Fukushima Cesium-137 radioactive plume. Deep Sea Res. I 93, 162–164.

Saad, Y., 1994. ILUT: a dual threshold incomplete LU factorization. Numer. Linear Algebra Appl. 1, 387–402.

Saito, Y., 1989. Late pleistocene coastal sediments, drainage patterns and sand ridge systems on the shelf off Sendai, northeast Japan. Mar. Geol. 89, 229–244.

SCJ, 2014. A Review of the Model Comparison of Transportation and Deposition of Radioactive Materials Released to the Environment as a Result of the Tokyo Electric Power Compny's Fukushima Daiichi Nuclear Power Plant Accident (Report of the Sectional Committee on Nuclear Accident Committee on Comprehensive Synthetic Engineering, Science Council of Japan).

Suh, K.S., Jeong, H.J., Kim, E.H., Hwang, W.T., Han, M.H., 2006. Verification of the Lagrangian particle model using the ETEX experiment. Ann. Nucl. Energy 33, 1159–1163.

Suh, K.S., Han, M.H., Jung, S.H., Lee, C.W., 2009. Numerical simulation for a long-range dispersion of a pollutant using Chernobyl data. Math. Comput. Model. 49, 337–343.

Takemura, T., Nakamura, H., Takigawa, M., Kondo, H., Satomura, T., Miyasaka, T., Nakajima, T., 2011. A numerical simulation of global transport of atmospheric particles emitted from the Fukushima Daiichi Nuclear Power Plant. SOLA 7, 101–104.

TEPCO, 2011a. http://www.tepco.co.jp/en/nu/fukushima-np/f1/index2-e.html.

TEPCO, 2011b. http://www.tepco.co.jp/en/press/corp-com/release/index1112-e.html.

Terada, H., Katata, G., Chino, M., Nagai, H., 2012. Atmospheric discharge and dispersion of radionuclides during the Fukushima Dai-ichi Nuclear Power Plant accident. Part II: verification of the source term and analysis of regional-scale atmospheric dispersion. J. Environ. Radioact. 112, 141–154.

Tsumune, D., Tsubono, T., Aoyama, M., Hirose, K., 2012. Distribution of oceanic ^{137}Cs from the Fukushima Daiichi nuclear power plant simulated numerically by a regional ocean model. J. Environ. Radioact. 111, 100–108.

Umlauf, L., Burchard, H., 2003. A generic length-scale equation for geophysical turbulence models. J. Mar. Res. 61 (2), 235–265.

van Ledden, M., 2003. Sand-mud Segregation in Estuaries and Tidal Basins PhD Thesis. Delft University of Technology, Delft, 221 pp.

van Rijn, L.C., 1984a. Sediment transport, Part I: bed load transport. J. Hydraul. Eng. 110, 1431–1456.

van Rijn, L.C., 1984b. Sediment transport, part II: suspended load transport. J. Hydraul. Eng. 110, 1613–1641.

Winterwerp, J.C., van Kesteren, W.G.M., 2004. Introduction to the Physics of Cohesive Sediment Dynamics in the Marine Environment. Elsevier, p. 576.

Zhang, Y., Battista, A.M., 2008. SELFE: a semi-implicit Eulerian-Lagrangian finite-element model for cross-scale ocean circulation. Ocean. Model. 21 (3–4), 71–96.